Accepted for publication at Atmospheric Research – please see final version at: https://doi.org/10.1016/j.atmosres.2020.105415

An overview of tornado and waterspout events in Catalonia (2000–2019)

Oriol Rodríguez [a,*], Joan Bech [a], Joan Arús [b], Salvador Castán [c], Francesc Figuerola [d], Tomeu Rigo [d]

[a] Department of Applied Physics – Meteorology, University of Barcelona, Barcelona, Catalonia, Spain
[b] DT Catalonia, Spanish Meteorological Agency, Barcelona, Catalonia, Spain
[c] Agencia Pericial, Cornella` de Llobregat, Catalonia, Spain
[d] Meteorological Service of Catalonia, Barcelona, Catalonia, Spain

ABSTRACT

Tornado climatologies are essential to enhance our knowledge about their frequency and spatial distribution, together with their damage path characteristics. Due to their small spatiotemporal scale, tornado detection is strongly linked to visual observations. Therefore, social networks have become one of the most important sources of severe weather reports during the present century, including tornadoes, improving their detection and increasing the number of observed cases compared to previous decades. This article presents an analysis of tornado and waterspout events reported between 2000 and 2019 in Catalonia (NE Iberian Peninsula), one of the southern European regions where these phenomena are most frequent. The study includes 105 tornadoes and 329 waterspouts reported in a 32,000 km^2 area, and therefore, it presents one of the highest tornado and waterspout densities in the Mediterranean basin according to recent climatologies. Remote-sensing tools such as weather radar, lightning detection and satellite imagery have been used to validate each event. Moreover, fieldwork performed after several tornado cases and the use of high-resolution aerial imagery have provided information to characterise damage paths, including the length and width of the damage swath and the maximum intensity according to the Enhanced Fujita Scale. Finally, a list of the analysed events is provided for further research.

1. Introduction

Tornadoes, which are the most intense wind phenomenon on Earth (AMS, 2020), occur mainly between 20° and 60° of latitude (Goliger and Milford, 1998). It is well known that central and eastern USA present favourable conditions for tornadic storms (Brooks et al., 2003; Taszarek et al., 2020), but in other parts of the world such as Europe they also occur frequently. Several significant events –i.e., F2/EF2 or stronger according to Fujita scale (Fujita (1981)) and Enhanced Fujita scale (WSEC (2006)) respectively– causing injuries and fatalities, have been reported across the continent throughout history (e.g., Gaya`, 2007; Holzer et al., 2018), as well as tornado outbreaks such as the 24–25 June 1967 (Antonescu et al., 2020), 23 November 1981 (Apsley et al., 2016) or 9 June 1984 (Chernokulsky and Shikhov, 2018).

Tornadoes, which are the most intense wind phenomenon on Earth (AMS, 2020), occur mainly between 20° and 60° of latitude (Goliger and Milford, 1998). It is well known that central and eastern USA present favourable conditions for tornadic storms (Brooks et al., 2003; Taszarek et al., 2020), but in other parts of the world such as Europe they also occur frequently. Several significant events –i.e., F2/EF2 or stronger according to Fujita scale (Fujita (1981)) and Enhanced Fujita scale (WSEC (2006)) respectively– causing injuries and fatalities, have been reported across the continent throughout history (e.g., Gaya`, 2007; Holzer et al., 2018), as well as tornado outbreaks such as the 24–25 June 1967 (Antonescu et al., 2020), 23 November 1981 (Apsley et al., 2016) or 9 June 1984 (Chernokulsky and Shikhov, 2018).

The first European tornado climatology was published during the second decade of the 20th centuranty by Wegener (1917), including 258 reports between 1456 and 1913 (Antonescu et al., 2019). Overtime, technological advances had contributed to the improvement of tornado detection, increasing the number of reports and making possible a better description of their temporal and spatial distribution. Recent climatologies show that in the Mediterranean basin there are some tornado density hotspots (Antonescu et al., 2017), probably related to local

complex topography enhancing mesoscale favourable conditions, as reported in several case studies (e.g., Homar et al., 2003; Matsangouras et al., 2014a, 2016; Miglietta and Rotunno, 2016). In Antonescu et al. (2017), Gay`a (2018) and Grieser and Haines (2020) it is shown that the maximum tornado frequency in the western Mediterranean is located between Catalonia and Balearic Islands.

Gaya` et al. (2011) provided the first analysis of tornado and waterspout occurrence in Catalonia, covering the 1950–2009 period. They identified the central part of the littoral as the area where tornado frequency is maximum. A similar pattern was found in Gay`a (2018), where the period of study was extended up to 2012. Occasionally, significant events have been reported in the region (Ramis et al., 1999; Aran et al., 2009; Bech et al., 2009, 2011; Pineda et al., 2011; del Moral et al., 2020a) and also tornado outbreaks have affected high-densely populated areas, such as Barcelona and Tarragona metropolitan areas (Bech et al., 2007; Mateo et al., 2009). The high socioeconomical impact of these events and their frequency have motivated the recent study of tornadic storms vertical profile characteristics (Rodríguez and Bech, 2018, 2020a) and, together with the occurrence of other severe weather phenomena, the development of nowcasting tools to predict severe thunderstorms (Farnell et al., 2017).

During the last two decades, the exponential use and dissemination of severe weather information on internet, smartphones and social networks, and even some movies such as “Twister” (Rauhala et al., 2012) increased the general interest in tornadoes all over the world. Moreover, the local improvement on radar coverage and data quality (Altube et al., 2015, 2017) and the installation of a lightning detection network (Pineda and Montanya`, 2009) in the early 2000 in Catalonia has also helped to better identify convective storms and severe weather events in the region of study. An increasing number of post-event surface damage surveys (Rodríguez et al., 2020) and the use of high-resolution aerial imagery on detecting tornado-related damage swaths (Rodríguez and Bech, 2020b) also contributed to enlarge the number of tornado and waterspout reports compared to the late 20th century.

The main goal of this article is to present a homogeneous and robust dataset of tornado and waterspout reports registered from 2000 to 2019 in Catalonia, analysing their main spatial and temporal features. This 20-year period is comparable to other recent tornado climatologies carried out in Europe (Matsangouras et al., 2014b; Miglietta and Matsangouras, 2018; Sioutas and Doe, 2019; Leita˜o and Pinto, 2020) and gathers results from technological advances on severe weather observations, decreasing the number of unreported events and providing a comprehensive updated analysis of one of the European tornado hotspots.

This paper is organized as follows. In Section 2 the region of study is presented and the tornado and waterspout database is introduced, detailing information sources and the validation and recording process of each event. Then, in Section 3 results are discussed, showing the spatial and temporal distribution of tornadoes and waterspouts, tornado outbreaks and multiple tornado or waterspout events, damage swath characteristics and socioeconomic impact in terms of injured people and damage loss estimation. Finally, in Section 4 a summary, conclusions and proposals for future work are presented. Moreover, an Appendix lists individual tornado and waterspout events analysed in this study (date and time, coordinates of touchdown and intensity rating) provided for open use in further studies.

2. Data and methodology

2.1. Region of study

Catalonia, which is located in the north-east of the Iberian Peninsula (Fig. 1), is a 32,000 km^2 region divided into 42 counties, with a population of 7.7 million (IDESCAT, 2020). Pyrenees and Pre-Pyrenees mountain ranges extend in the north, from east to west, with peaks exceeding 3100 m and 2600 m, respectively. Moreover, parallel to the coast there are the Littoral (700 m) and Pre-Littoral (1700 m) mountain ranges with flat areas between them, whereas western Catalonia is dominated by the Ebro depression, which is a large flat area. The interaction of complex topography with low-level moist-warm air from the Mediterranean Sea and upper-level cold air advections from higher latitudes produces –mainly during the warm season– severe convective storms (Calvo-Sancho and Martín, 2020; Martín et al., 2020), sometimes with large hail (Farnell et al., 2009), strong winds (Lo´pez, 2007) and

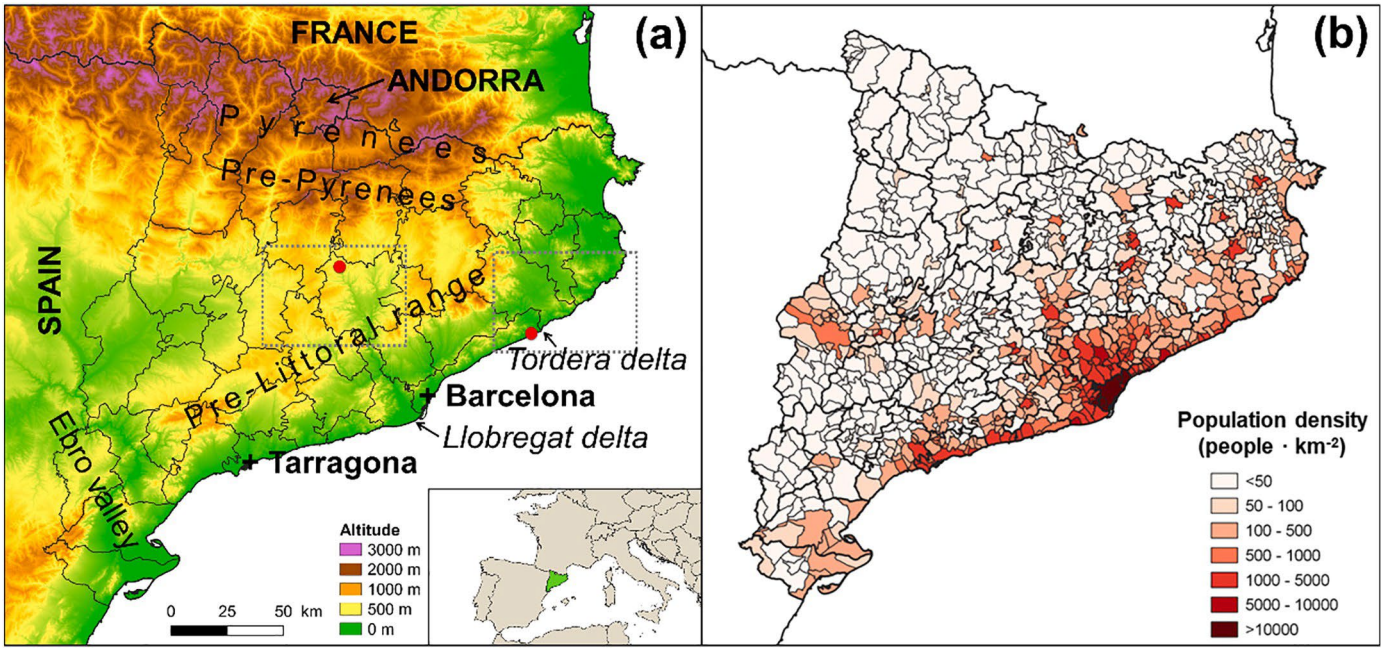

Fig. 1. (a) Topographical map of Catalonia showing Barcelona and Tarragona cities, and Tordera and Llobregat deltas location. County borders are indicated with thick black lines. Moreover, the selected area of the cases shown in Fig. 4 is marked with grey-dotted rectangles and tornado location is indicated with red dots. The insert, shows the location of the region of study (shaded in green) in SW Europe. (b) Municipal population density map of Catalonia (source of data: Cartographic and Geologic Institute of Catalonia ICGC and Statistics Institute of Catalonia IDESCAT).

tornadoes.

2.2. Tornado and waterspout database

The tornado and waterspout database consists of 434 individual vortices (i.e., a tornado or a waterspout) observed from 2000 to 2019 in Catalonia and the surrounding sea area. The database follows the *Glossary of Meteorology* (AMS, 2020) definition for tornado "A rotating column of air, in contact with the surface, pendant from a cumuliform cloud, and often visible as a funnel cloud and/or circulating debris/dust at the ground" (105 (24%) cases in the dataset) and waterspout "In general, any tornado over a body of water" (329 (76%) events). In the database, waterspouts that make landfall are considered tornadoes, representing 41 (39%) of tornado events. As indicated above, note that in this article the term vortex is used to refer to individual tornadoes or waterspouts, not to rotating structures within a tornado as in other studies (Wurman et al., 2014).

Generally, for each tornado, date, hour, location (i.e. latitude, longitude, and affected municipalities and counties) and the intensity estimation using the EF-scale (WSEC, 2006) are provided. If available, starting and ending latitude and longitude of damage track, the damage path length and width, the number of injuries and fatalities and the damage loss estimation are also recorded. For waterspout events (e.g., Fig. 2) date, hour, and location are registered.

2.3. Sources of tornado and waterspout reports

Reports of tornadoes and waterspouts have been collected from meteorological spotters and casual witness observations, emergency services (firefighters, police and civil protection) and mass media during all the period of study. Furthermore, the internet and social networks have become a crucial source of unusual meteorological observations hardly captured by operational observing networks (Hyva¨rinen and Saltikoff, 2010; Grasso et al., 2017), particularly in severe weather events (e.g., Kahraman and Markowski, 2014; Kirk, 2014; Rigo and Farnell, 2019; Chernokulsky et al., 2020), being an essential source of information about tornadoes and waterspouts during the second decade of the period of study (Fig. 3). This is reflected in the creation, during the last years, of several citizen collaborative platforms such as the European Severe Weather Database (ESWD; Dotzek et al., 2009) from the European Severe Storms Laboratory (ESSL), the Reporting System of Singular Atmospheric Observations (SINOBAS; Guti´errez et al., 2015) from the Spanish Meteorological Agency (AEMET) and the Meteorological Spotters Network (XOM; Ripoll et al., 2016) from the Meteorological Service of Catalonia (SMC); the three platforms provided part of tornado and waterspout reports included in the database. All this information was combined with the catalogue of tornadoes and waterspouts of Spain described by Gay`a (2018), which contains cases up to 2012.

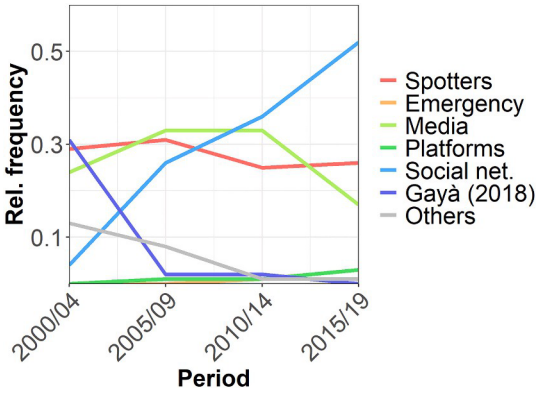

Fig. 3. Relative frequency of selected report sources: meteorological spotters, emergency services, media, citizen collaborative platforms, social networks, Gaya` (2018) and others for each 5-year windows during 2000–2019.

2.4. Validation and recording of reported events

A validation process is necessary to avoid introducing erroneous or duplicated reports into severe weather databases (Dotzek et al., 2009). The validation followed here to build up the database consists of two steps:

1. Confirming that atmospheric convection was present during the day and time of the reported event
2. Confirming that damage was really caused by a tornado instead of other strong winds of convective origin (in case of reported damage and if no images of the funnel cloud and/or swirling debris are available).

The first step is carried out making a visual analysis of satellite data, C-band Doppler radar observations (Altube et al., 2015, 2017) and lightning data (Pineda and Montanya`, 2009) from the SMC, according to geographical and temporal information of each report. The main goal is to identify the parent-convective storm that spawned the tornado or the

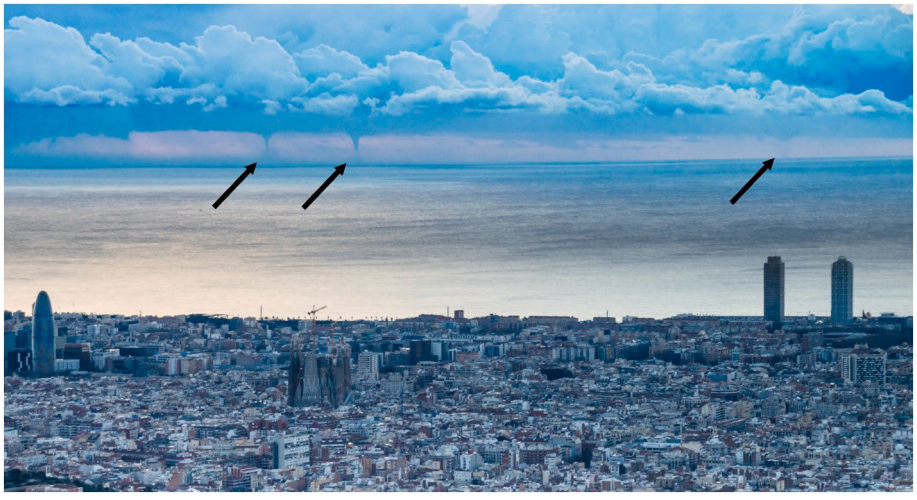

Fig. 2. Three waterspouts (indicated with black arrows) formed around 50 km off-coast in front of Barcelona, during the 7 March 2018 waterspout outbreak. Author: Alfons Puertas.

waterspout. Weather radar imagery is of special interest, as it may reveal classical features associated to supercell storms (Wilson et al., 1980; Zrni´c et al., 1985) either in the radar reflectivity field such as hook-echoes or on radial Doppler wind fields such as mesocyclonic velocity couplets (Fig. 4a), although in many cases these features may not be detectable (Fig. 4b) or simply they may not be present in case of non-mesocyclonic tornadoes (Wakimoto and Wilson, 1989). On the other hand, it should be taken into account that waterspouts can be associated with fair weather conditions (i.e., light- or non-precipitation nor lightning; Matsangouras et al., 2017; Miglietta, 2019), making possible the identification of the parent-convective storm only using satellite imagery such as infrared (10.80 μm) or visible (0.60 μm) channels. With this analysis it is generally feasible to estimate the timing of the event (usually with an uncertainty lesser than 5 min) and even the approximate location of waterspouts over the sea. This task was performed manually so it was time-consuming and, occasionally, results were inconclusive due to unavailable data (especially during the first five years of study) or, in case of extensive and long-lived convective systems, when it was not possible to identify the particular parent-storm.

The confirmation of tornado occurrence instead of other damaging winds of convective origin, in case no image of the phenomenon was available (step 2), is performed after mapping and examining the reported damage of each event. Consequently, this step is not carried out for waterspouts remaining all their life-cycle offshore. The information used to fulfil this analysis has been gathered by performing in-situ damage surveys (Rodríguez et al., 2020), when it has been possible. Therefore, 37% reported tornadic events between 2000 and 2009 and 63% of cases between 2010 and 2019 have been analysed in-situ (e.g., Bech et al., 2011; Bech et al., 2015). Moreover, 25 and 50 cm-spatial resolution orthophotographs from the Cartographic and Geologic Institute of Catalonia (ICGC) have been also used to assess damage swaths (Rodríguez and Bech, 2020b), looking for changes on forest coverage and on human-made structures comparing images taken before and after events, similarly to Karstens et al. (2010), Molthan et al. (2014, 2020) and Shikhov and Chernokulsky (2018). The study of damage patterns in forest areas (i.e., direction of fallen trees) can provide valuable clues for distinguishing damage caused by tornadoes, downbursts or straight-line winds (Fujita, 1981; Bech et al., 2009; Rhee and Lombardo, 2018). Long-narrow tracks with a convergent or rotational damage pattern and great damage gradient are compatible with tornadoes, whereas short-wide, divergent damage swath with a lesser damage gradient are more likely associated with downbursts (Bunting and Smith, 1993).

Then, only those cases for which all the validation process is completed are introduced in the database. Furthermore, the information recorded for each event is complemented by characterising the damage swath, when the identification of the track is possible. This analysis has been performed using data gathered during fieldworks and orthophotograph imagery, but also using information provided by emergency services and local authorities about geolocated damaged elements. On the other hand, data about injuries and fatalities has been obtained from

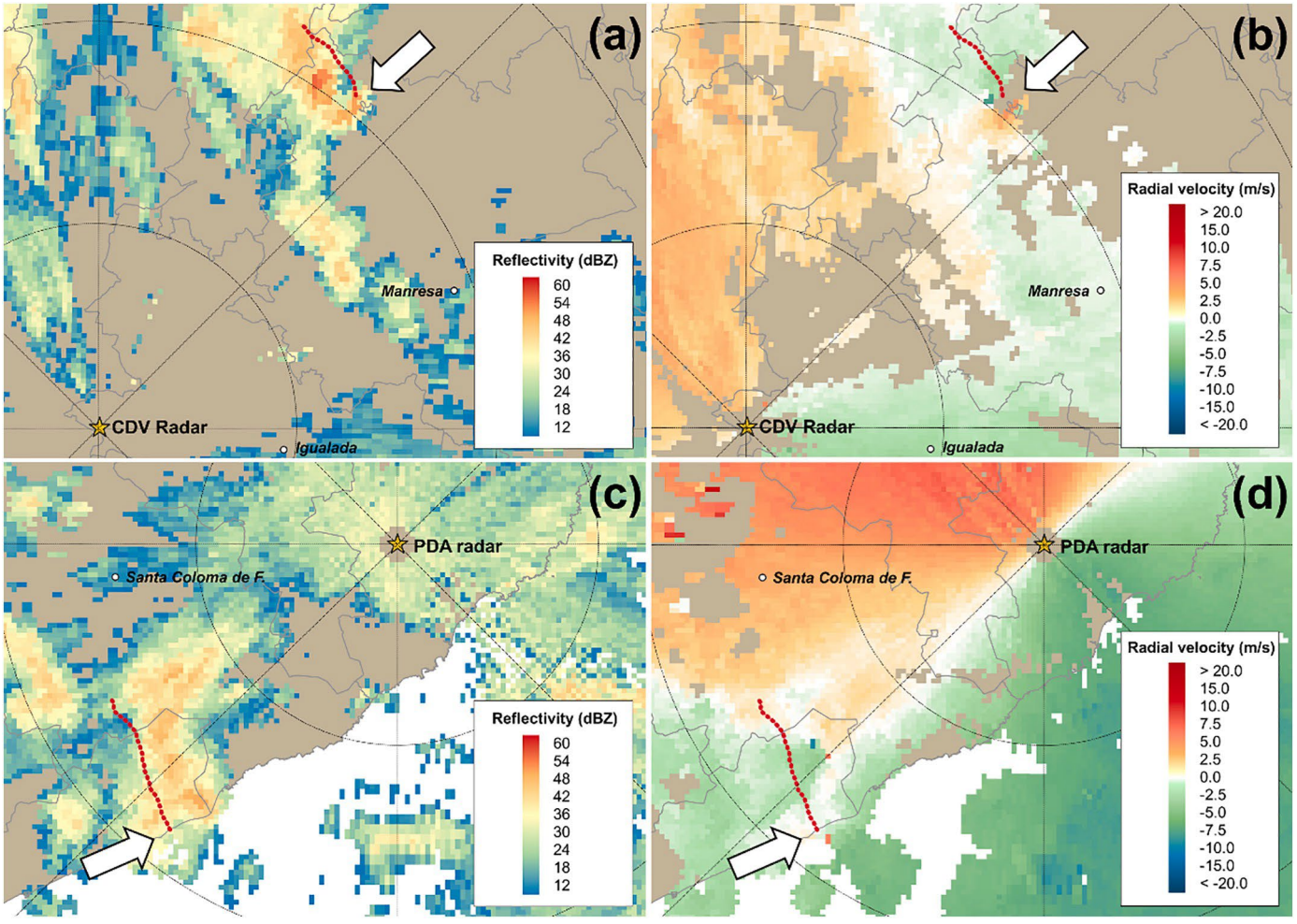

Fig. 4. Radar reflectivity (left column) and radial Doppler velocity (right column) weather radar PPIs (0.6° antenna elevation). Panels (a) and (b) were observed by the CDV radar (41.60° N, 1.40° E) on 7 January 2018 at 0054 UTC and panels (c) and (d) by the PDA radar (41.89° N, 3.00° E) on 15 October 2018 at 0136 UTC. Images show radar locations (stars), county capitals (white dots), tornado tracks (red-discontinuous lines), parent-storms (white arrows), and 20-km range rings and azimuths centred on each radar.

media.

Finally, the maximum intensity of each event has been estimated. To carry out this task we analysed damage observed in photographs from media and from fieldwork when performed. For each relevant element damaged, the EF-scale to assess wind intensity has been applied, proceeding as in Bech et al. (2015). The EF-scale consists of 28 damage indicators (type of construction or element, such as mobile homes, hospitals or trees) and 3 to 12 degree of damage for each one. Combining both parameters, a wind velocity range is given, which can be related to EF categories (WSEC, 2006; Mahieu and Wesolek, 2016). In contrast, F-scale, which was broadly used before 2007, is based on typical damage descriptions associated with F0 to F5 categories (Fujita, 1981). Therefore, the EF-scale makes possible a more detailed damage intensity rating instead of the original F-scale, despite limitations on its use specially outside the USA (Doswell III et al., 2009).

2.5. Damage loss estimation

Achieving realistic data of direct tornado damage loss is a non-trivial task; see for example discussions in Edwards et al. (2013) or Antonescu et al. (2017). In the present article, damage loss estimation has been carried out using data from the *Consorcio de Compensacio´n de Seguros* (CCS), local administrations and expert assessment. CCS provided damage compensation data, as it is the public reinsurance company of Spain which covers the damage to insured properties due to several natural disasters, including tornadoes since 2004. Due to policy coverage limitations, there is a difference of 13% between the compensation assumed by the insurance company throughout the CCS and the real cost of the damage (Martínez-Gomariz et al., 2019). Therefore, a correction factor based on this figure has been applied to CCS data to estimate the real insured properties damage cost caused by tornadoes.

Nevertheless, apart from the absence of tornado damage compensations data before 2004, there is also a lack of data for several events. This may be either by damage on uninsured properties (and therefore not covered by the CCS) or because the event caused minor or no damage which was not claimed to the CCS.

Damage loss estimation carried out by local administrations has also been used to complement the present analysis. These data have been taken into account instead of CCS data when this estimation was higher and when there were no CCS data for an event. This situation is especially common in rural areas where the ratio of uninsured properties is notably higher than in urban areas.

Finally, in case of no data availability from CCS nor local administrations, data from an expert assessment has been used, derived from the analysis of information gathered during in-situ damage surveys, similarly to Martínez-Gomariz et al. (2020). All these data have been converted to 31 December 2019 reference value to enable a consistent comparison.

3. Results and discussion

3.1. Spatial distribution

Tornado density in Catalonia is 1.65 tornadoes year^{-1} 10^{-4} km^{-2}, which is similar to Colorado (1.54) and Ohio (1.75) states in the USA, slightly higher than other Mediterranean countries such as Italy (1.23) or Greece (1.20), and higher than other European countries (Table 1). Nevertheless, the UK (1.92) is the European state where tornado density is the highest, although this value is far from the US Great Plains, reaching the maximum in Kansas (4.45 tornadoes year^{-1} 10^{-4} km^{-2}). If only significant events (i.e., EF2 or stronger according to the EF-scale, WSEC, 2006 – see Section 3.4) are taken into account, then the density is 0.13 events year^{-1} 10^{-4} km^{-2} in the region of study. As stated in Table 1, this value is slightly smaller than those reported in Ohio (0.21), Germany (0.19) or Portugal (0.19), and clearly smaller than in Kansas (0.37). In contrast, it is higher than for Italy (0.08) or Colorado (0.05). Similarly, the density of waterspouts normalized per year and 100 km of coastal line in Catalonia is 5.0, which is higher than in Croatia (3.0, Renko et al., 2016), in Greece (2.1, Matsangouras et al., 2014b), in Germany (2.1, Kühne et al., 2017), in Italy (0.9, Miglietta and Matsangouras, 2018) and in Portugal (0.2 in mainland, Leita˜o and Pinto, 2020). Nevertheless, if only near-coastal waterspouts are considered (i.e., located less than 10 km offshore), the density decreases to 2.7, which is similar to some of the previous-mentioned countries.

The spatial distribution of tornadoes is not homogeneous throughout the region of study (Fig. 5a). The highest density is found on the littoral and the pre-littoral, especially the central sector, being coherent with previous studies (Gaya` et al., 2011; Gay`a, 2018). There are some hotspots close to delta rivers such as Tordera and Llobregat (indicated in Fig. 1a) and also in the flat area surrounding Tarragona, where several waterspouts were reported to landfall. In those regions the mean number of events per year in 0.2° grid cells is between 0.40 and 0.55 (i.e. around one tornado every 2 years). Moreover, a few isolated cases have been observed in the rest of Catalonia, and only a couple has been reported in the Pyrenees and Pre-Pyrenees during the period of study.

The waterspout spatial distribution follows a similar pattern than that of coastal tornadoes, with maximum density between Barcelona and Tarragona, where between 1 and 2 events per year are reported in coastal grid cells (Fig. 5b). However, in both extremes of the littoral, especially in the northern one, the waterspout density is significantly lower. It is noticeable that the central area of the littoral and pre-littoral is the most populated area of the region of study (Fig. 1b). In this 4800 km^2 area (15% of Catalonia surface) live 5.6 M inhabitants (73% of the population). Therefore, an important question here is: is there a bias on tornado spatial distribution caused by population density?

To answer this question, we reviewed previous research in the region of study devoted to the analysis of the spatial distribution of lightning strikes and convective storm structures –both independent from population density–, and hailstorms, assuming that tornadoes are usually related to deep-moist convection. Even though, it should be taken into account that in some occasions, they can be formed within fair weather

Table 1
Tornado density, significant tornado density, period and reference of data for selected USA States and Countries.

State / Country	Period	Tornado density (y^{-1} 10^{-4} km^{-2})	Significant tornado density (y^{-1} 10^{-4} km^{-2})	Reference
Kansas	2000–2018	4.45	0.37	NOAA/SCP (2019)
United Kingdom	1981–2010	1.92	–	Kirk (2014)
Ohio	2000–2018	1.75	0.21	NOAA/SCP (2019)
Catalonia	2000–2019	1.65	0.13	This article
Colorado	2000–2018	1.54	0.05	NOAA/SCP (2019)
USA	2000–2018	1.24	0.13	NOAA/SCP (2019)
Italy	2007–2016	1.23	0.08	Miglietta and Matsangouras (2018)
Greece	2000–2019	1.20	–	Sioutas and Doe (2019)
Germany	2002–2016	1.12	0.19	Kühne et al. (2017)
Portugal (mainland)	2001–2019	0.67	0.19	Leita˜o and Pinto (2020)

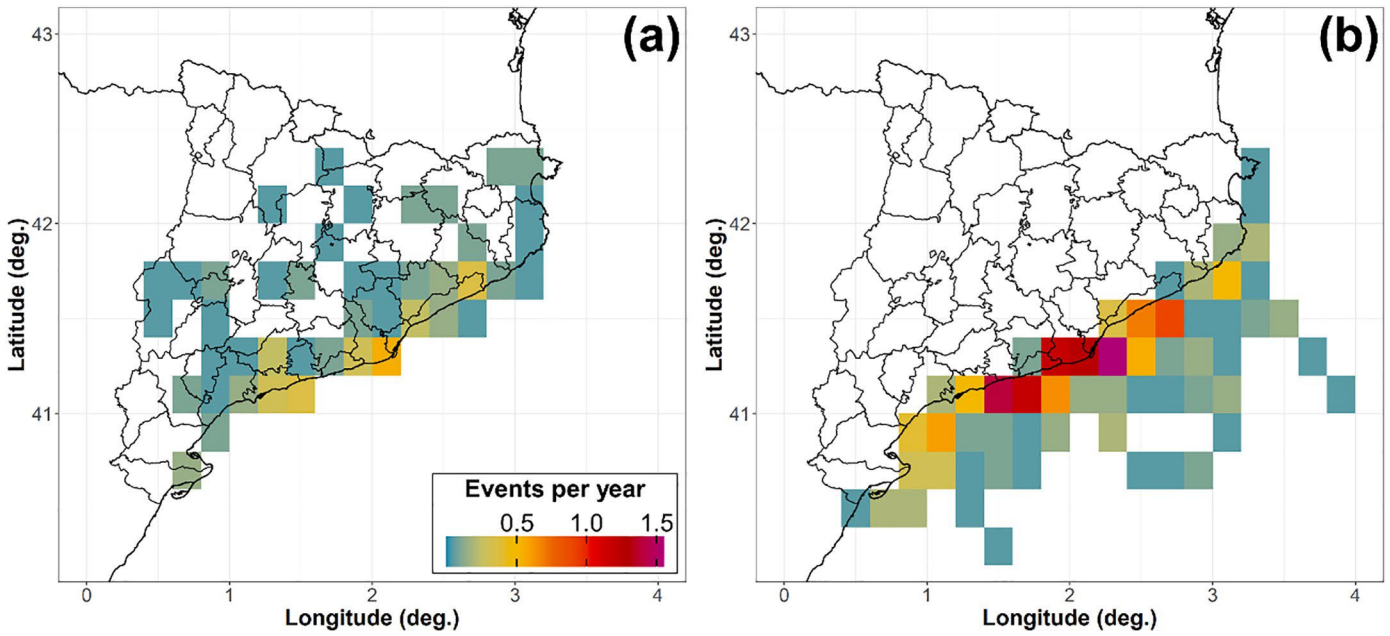

Fig. 5. Number of tornadoes per year, based on initial touchdown (a), and number of waterspouts per year (b) in a 0.2° per 0.2° grid.

conditions mainly offshore, limiting partially the following discussion.

In Pineda and Soler (2015) it is shown that the maximum lightning density (more than 3 cloud to ground flashes year^{-1} km^{-2}) is located in the Pre-Pyrenees, especially in the central and eastern sector. It coincides with the area where hailstorms (Rigo and Farnell, 2019) and convective storm structures (del Moral et al., 2017) frequency is the highest, pointing out this subregion as the most favourable for deep convection. Nevertheless, this area does not present the highest tornado density, as previously described. The low number of reported events in Pyrenees and Pre-Pyrenees could be explained by complex topography, which reduces the visibility, and the low population-density, hindering the direct visual observations (Schuster et al., 2005; Saltikoff et al., 2010; Potvin et al., 2019). Moreover, the lightning monthly distribution could also provide another explanation for that. According to Pineda and Soler (2015), the thunderstorm season in this subregion starts on late spring and finishes on late summer, and their formation is usually related to the diurnal heating cycle combined with sea surface temperature seasonal cycle (Pastor et al., 2018) and upslope breezes (Callado and Pascual, 2005). During warm season, Jet Stream and associated surface lows are weaker and move farther north (Koch et al., 2006), favouring low-shear environments in the region, whereas tornadic storms are usually associated with moderate to high shear and helicity conditions, especially in low-levels (Taszarek et al., 2017; Rodríguez and Bech, 2018, 2020a). Therefore, the lack of environments with instability overlapping with high shear could hamper tornado formation in Pyrenees and Pre-Pyrenees.

On the other hand, lightning density presents a secondary maximum in the Tarragona area, extending north-east in front of the coast up to Barcelona (del Moral et al., 2020b), whereas in northern littoral there is a minimum. This distribution is related with northern surface synoptic wind situations, when the orographic effect of the Pyrenees favours the formation of a convergence zone in the central Catalan littoral between the tramontane flow from the northern coast and the mistral flow in the southern region, which is channelled by the Ebro valley (Pen˜a et al., 2011; Gonzalez et al., 2018). In case of vertical instability, the presence of a convergence line can initiate convection, and furthermore can support waterspout formation (Miglietta, 2019). Therefore, it could explain the tornado and waterspout maximum in the central sector of the littoral and pre-littoral, although population distribution may also contribute to draw the pattern shown in Fig. 5b.

3.2. *Temporal distribution*

Between 5 and 6 tornadoes are reported in 3 to 4 days every year on average in Catalonia, which provides a ratio of 1.4 tornadoes per tornadic day (i.e. a day with at least one tornado reported). The number of waterspouts per year is notably higher, between 16 and 17, observed in 9 to 10 days. Thus, the number of waterspouts per waterspout day (i.e. a day with at least one waterspout reported) is 1.8, being comparable to other Mediterranean countries such as Greece (1.7, Sioutas and Doe, 2019) or Croatia (2.4, Renko et al., 2016). Even so, the yearly tornado and waterspout standard deviation is 3.3 and 10.2, respectively, which indicates that there is a large interannual variability, as shown in Fig. 6a, b. Thus, the number of tornadoes per year ranges from 1 tornado in 2000 to 13 in 2018 and the annual number of waterspouts, from 3 in 2000 to 38 in 2016. On the other hand, the annual numbers of tornado days and waterspout days are more homogeneous (Fig. 6c), presenting a yearly standard deviation of 2.3 days and 4.0 days, respectively. This difference on annual behaviour between the number of individual tornadoes and waterspouts and the number of days when they were observed, especially for the latter, is because of the occurrence of multiple events and outbreaks. These events can occasionally generate more than 5 tornadoes or waterspouts in a single day (see Section 3.3 for further discussion).

Interestingly, it can be observed that, whereas 65% of reported tornadoes between 2000 and 2009 were rated as EF0, the percentage raised up to 80% for the next ten years, a figure consistent with previous studies (e.g., Verbout et al., 2006; Gay`a, 2018). Moreover, 42% of those EF0 reported during the first decade were mainly concentrated in the five most populated counties, whereas between 2010 and 2019 it was only 29%. Similarly, the ratio of waterspouts observed far-away from the coast (i.e., 10 km or more offshore) also increased from 27% for the first decade to 53% for the second. These differences are a consequence of the improvement of the detection of low-impact events (weak tornadoes and far-offshore waterspouts) during the period of study. As explained in Section 2.3, the expansion of internet and social networks, the increasing number of smartphones, the consolidation of remote-sensing networks, the growing interest on severe weather, together with the increase of Catalonia population from 6.2 M inhabitants in 2000 to 7.7 M people in 2019 (IDESCAT, 2020) have likely contributed to a better observation of this kind of events.

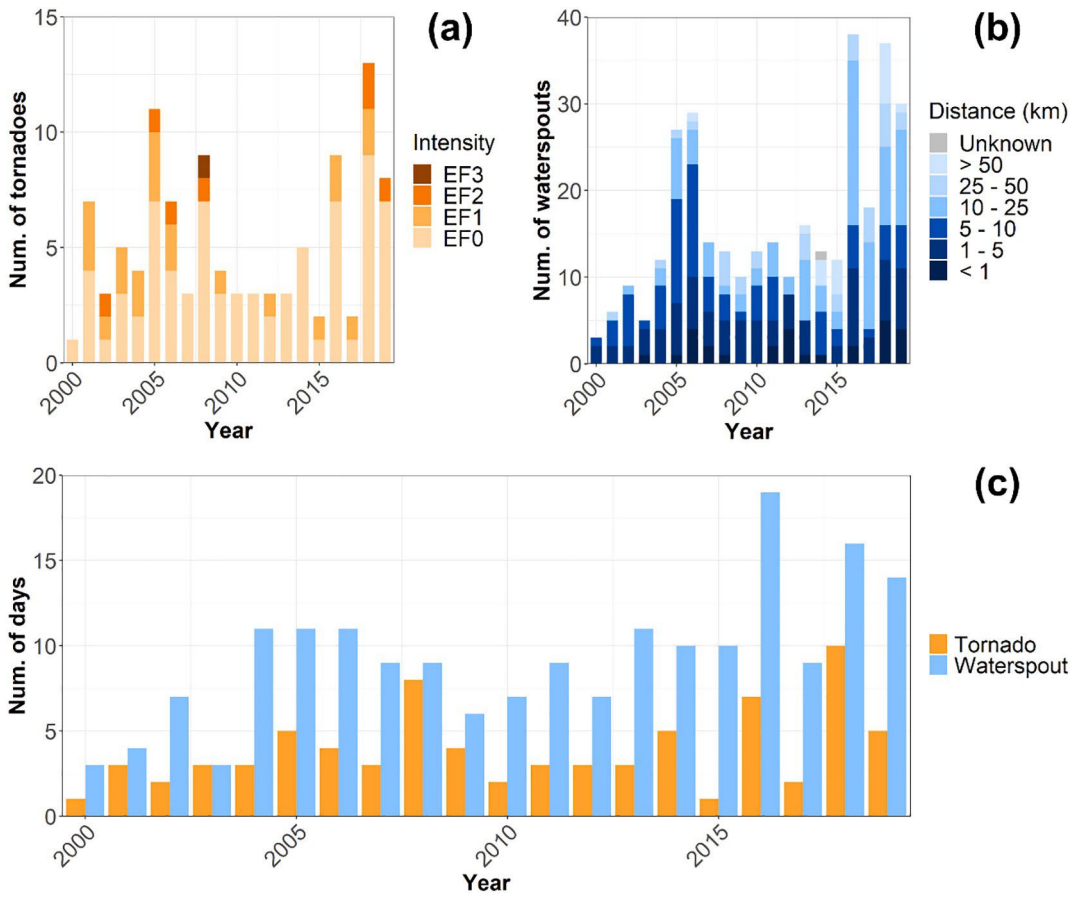

Fig. 6. Number of tornadoes depending on their intensity (a), number of waterspouts depending on their distance from the coast-line (b), and number of tornado days and waterspout days (c) per year reported between 2000 and 2019.

Both tornado and waterspout events have a similar seasonal and monthly distribution (Fig. 7). Although they can occur at any time of the year, a vast majority have been observed in autumn (56% of tornadoes and 60% of waterspouts) and in summer (19% and 21%). In contrast, winter (10% and 9%) and spring (15% and 10%) are the less favourable seasons for their occurrence. The tornado season in the area of study runs from August to November (69% of the tornadic cases), reaching the peak in October. On the other hand, a secondary tornado activity maximum is observed between April and May (12%). This result is similar to that previously found by Gay`a et al. (2011), although the maximum has been shifted towards autumn. The monthly distribution presented here is similar to other Mediterranean countries such as Greece (Matsangouras et al., 2014b) or Italy (Miglietta and Matsangouras, 2018), but differs from central and northern Europe, where

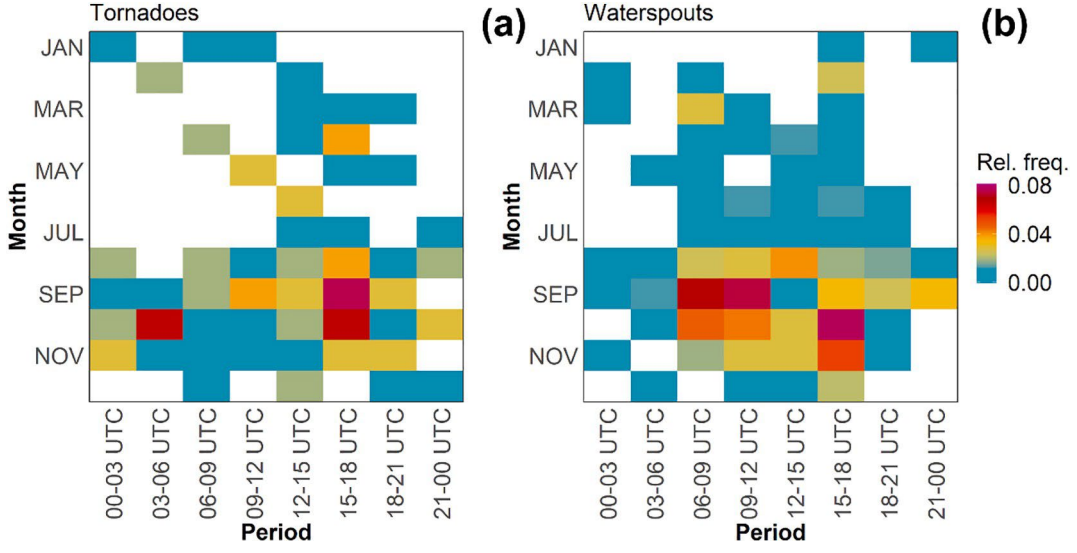

Fig. 7. Hourly and monthly relative frequency of tornadoes (a) and waterspouts (b).

tornadoes are usually observed between June and August (Groenemeijer and Kühne, 2014; Antonescu et al., 2016). Differences between central and northern Europe and the region of study can be explained by the influence of the Mediterranean Sea shifting the maximum convective activity towards autumn and the more frequent presence of the jet stream later in the season compared to higher latitudes. Regarding waterspout seasonal patterns, 75% of waterspouts are also reported during the August to November period, but the most active month is September.

The hourly distribution of tornadic events in the area of study (Fig. 7a) shows that they are more common during afternoon (especially between 15 and 18 UTC), when 44% (29%) of the reported cases were detected. This pattern, which is comparable to that for inland lightning strikes presented in Pineda and Soler (2015), can be explained by the diurnal solar heating cycle, that supports deep convection and tornadogenesis as stated in other studies for several regions (e.g., Kirk, 2014; Chen et al., 2018; Chernokulsky et al., 2020). In contrast, some differences are observed when our results are compared to Gaya` et al. (2011) findings, where a secondary maximum on tornado activity was presented between 09 and 12 UTC (not observed here) and the highest tornadic events frequency was detected during early afternoon instead of the late-afternoon. These differences might be due to the smaller size of the sample data of the above-mentioned study (54 tornadoes) respect to the 105 hourly-determined events analysed here.

Unsurprisingly, waterspouts are mostly observed also during the diurnal period (Fig. 7b) which could be expected given their mostly visual detection. Their hourly distribution presents two maxima: during the morning (06–12 UTC) and in the late afternoon (15–18 UTC). This pattern, with a relative minimum during early afternoon (12–15 UTC), is consistent with previous works (Gaya` et al., 2011) and also with the Balearic Sea lightning hourly distribution (Pineda and Soler, 2015), which presents a decay on the number of strikes during this 3-h window.

The lowest tornado and waterspout frequency is observed during the nocturnal period, between 21 and 06 UTC, when only 25% tornadoes and 10% waterspouts have been reported. The lack of visibility due to the darkness and the smaller number of potential eye-witness during night (Potvin et al., 2019) contribute to draw this pattern. Moreover, meteorological factors such as inland thunderstorm daily cycle activity also presents the daily minimum during this period (Pineda and Soler, 2015), supporting the low frequency of nocturnal tornadic events. In contrast, the highest occurrence of offshore lightning events is observed during night, which does not fit with the small number of waterspouts detected during darkness hours. Therefore, that discrepancy could suggest that nocturnal waterspouts are more underreported than nocturnal tornadoes.

3.3. *Outbreaks and multiple events*

The Glossary of Meteorology (AMS, 2020) defines tornado outbreak as "multiple tornado occurrences associated with a particular synoptic-scale system". Nevertheless, some authors restrict the term tornado outbreak for those events in which 5 or more (Pautz, 1969), 6 or more (Galway, 1975) or 10 or more (Galway, 1977) tornadoes are reported, whether others such as Hagemeyer (1997) also presents a temporal-window restriction (4 or more tornadoes in a lapse time of 4 h or less). In this section, we follow Galway (1975) outbreak definition, but taking both tornado and waterspout occurrences into account. According to the classification presented in the previous-mentioned article, in terms of number of tornadoes per outbreak, there are three main outbreak classes: small (6 to 10), moderate (11 to 20) and large (more than 20).

From 2000 to 2019 75 events with 2 or more individual tornados or waterspouts have been registered in Catalonia, 17 of which can be considered outbreaks (Fig. 8). The vast majority of them (82%) were small, 2 were moderate and 1 was large. The most extensive one was on 7 and 8 September 2005, when at least 21 individual vortices (7

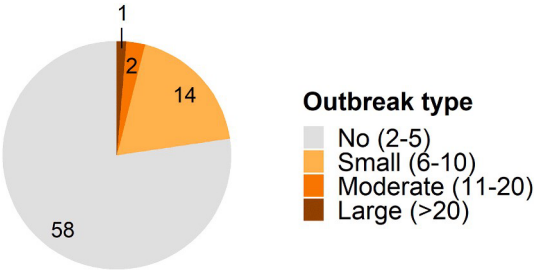

Fig. 8. Frequency of tornado outbreak type, according to Galway (1975) categories ("Small outbreak", "Moderate outbreak" and "Large outbreak") including both tornadoes and waterspouts. "No-outbreak" type includes events in which 2 to 5 vortices formed in the same synoptic-scale system.

tornadoes and 14 waterspouts), the strongest one rated as an EF2, mainly affected the Barcelona international airport and its surrounding area (12 km SW Barcelona, in Llobregat delta), causing the interruption of air traffic operations for 1 h (Bech et al., 2007). The low number of moderate and large outbreaks could be explained by the relatively small size of the area of study compared to similar researches.

The duration of outbreaks is higher than those presented in previous studies for other countries (e.g., Galway, 1977). The average is 27 h, and the median 25 h. The main reason is that they usually occur when a cut-off low is located in the centre or south of the Iberian Peninsula, which is a synoptic situation that can persist for some days (e.g., Romero et al., 2000; Homar et al., 2002).

In some occasions, several tornadoes or waterspouts may be formed by a single convective storm and sometimes they can be observed simultaneously (Sioutas et al., 2013; Miglietta et al., 2020), being more common for waterspouts (see Fig. 2 as an example). In order to analyse these cases, a multiple event is defined here as the one where two or more tornadoes or waterspouts formed within a particular convective storm during its life cycle.

The database reveals that 158 vortices have been observed during 54 multiple events, 13 corresponding to tornadoes and 145 to waterspouts. The mean elapsed time between the formation of the first and the last reported vortex is 30 min, although 6% of cases exceeded 1 h. In 52% of them, two vortices where reported, and only in 7% of them more than 5 individual vortices were formed (Table 2), a figure similar to the one reported for Italy by Miglietta and Matsangouras (2018). The two largest events occurred on 7 September 2005 between 1715 and 1818 UTC, when 4 tornadoes and 4 waterspouts affected the Llobregat delta, and on 7 March 2018 between 0613 and 0646 UTC, when 8 waterspouts formed around 50 km off-coast in front of the central Catalan littoral area (Fig. 2).

The number of reported multiple events has increased during the period of study. Between 2000 and 2009 21 cases were detected, whereas between 2010 and 2019 the number raised up to 33. This difference is related to the increasing number of available images of reported events and the ease to contact with their authors, facilitating the identification of non-simultaneous tornadoes or waterspouts formed

Table 2
Frequency of multiple events reported from 2000 to 2019 depending on the number of vortices (individual tornado or waterspout) formed by a particular convective storm.

Number of vortices	Frequency
2	28
3	15
4	6
5	1
6	2
7	0
8	2

within the same convective storm.

3.4. Damage path characteristics

Damage assessments classified 72% tornadoes as EF0, 20% as EF1 and 8% as EF2 or stronger. Only one EF3 event has been observed during this 20-years period, registered on 2 November 2008 30 km northern Tarragona (Rodríguez and Bech, 2020b). The percentage of EF0 is clearly higher than in previous studies (43% in Gay`a et al., 2011), whereas the ratio of EF1 is significantly smaller (44% in that work). This could be explained by the differences between the period of study of the above-mentioned works, which extends between 1950 and 2009, and the analysed here. As stated in Section 3.1, smartphones, internet and social networks, among others, have favoured reporting weak events compared to decades ago, increasing the percentage of EF0 tornadoes on databases (e.g., Verbout et al., 2006).

Despite the lack of violent events (i.e., EF4/EF5), the proportions presented here show some similarities to USA tornadoes (Fig. 9). Nevertheless, it can be observed that, whereas the ratio of EF0 in Catalonia is higher than in the USA, the proportion of EF1 is smaller. That could be explained by the high number of tornadoes formed offshore in the dataset (39% of the total), which are usually non-mesocyclonic (Markowski and Richardson, 2009). Therefore, whereas, 78% of waterspouts making landfall have been rated as EF0, 17% as EF1 and 5% as EF2+, 68% of formed-inland events have been rated as EF0, 22% as EF1, and 10% as EF2+, being this second distribution more similar to the USA data (not shown).

Around 42% of the analysed damage paths are shorter than 1 km. From them, more than a half correspond to tornadoes formed offshore that weaken when move onshore. The vast majority of tornado tracks are smaller than 5 km (82%), and only 7% are larger than 10 km, being consistent with previous studies (Gay`a et al., 2011; Gaya`, 2018). The longest damage path in the database is 45.5 km, which corresponds to the 7 January 2018 tornado, formed in NE Catalonia (Rodríguez et al., 2018). Comparing these results to the USA data (NOAA/SPC, 2019), it is noteworthy that, in general, damage swaths are longer than in Catalonia (i.e., 73% are shorter than 5 km and 14% are longer than 10 km).

Similarly to short damage tracks, the narrowest paths are usually related with waterspouts that move onshore. Then, more than 50% of the 50 m or less-wide swaths are due to tornadoes formed over the sea. 79% of the studied damage paths are narrower than 200 m, and only occasionally are wider than 500 m (6% of the cases). Proportions presented here are similar to the USA data, where 85% of tornado tracks do not overcome 200 m width and only 4% of them exceed 500 m.

Furthermore, stronger tornadoes are usually related with longer and wider damage paths than weaker tornadoes. Brooks (2004) reported a statistical relation based on Weibull distribution between tornado intensity (there, using the F-scale, Fujita, 1981) and length and width of tornado path with data from the USA. As presented in Fig. 10, the track length of weak tornadoes is generally smaller than 10 km, whereas the majority of significant events surpass this threshold. Regarding the damage swath width, while very few weak tornadoes produce a path wider than 200 m, EF2+ events mostly exceed 400 m width. The 50th percentile of track length and width for EF0 is 0.6 km and 35 m, for EF1 is 3.9 km and 145 m, and for EF2+ is 12.4 km and 485 m.

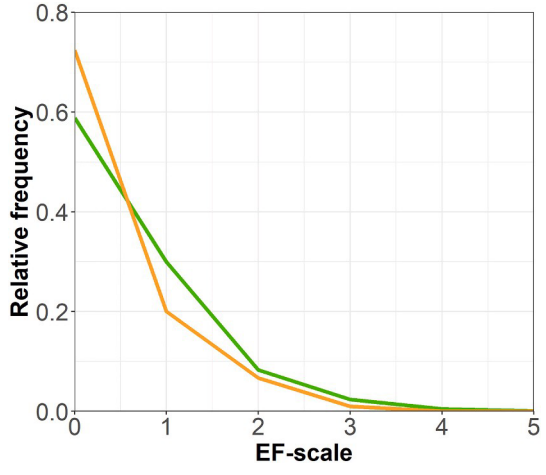

Fig. 9. Relative frequency of tornadoes depending on their intensity according to EF-scale in Catalonia (orange) and USA (green, NOAA/SPC, 2019).

Tornado damage tracks are usually oriented from south to north and present differences depending on their origin. Fig. 11 shows orientation distributions for tornadoes formed inland (a) and offshore (b). Tornadoes which touchdown inshore, usually move from the 3rd quadrant to the 1st (49%) and from the 2nd quadrant to the 4th (33%), although the predominant directions of movement are SSW to NNE (20%) and SSE to NNW (18%). This pattern has also been observed in other Mediterranean countries such as Greece (Sioutas, 2011) or Italy (Miglietta and Matsangouras, 2018). On the other hand, waterspouts can make landfall when move perpendicular to the coast, which is mostly oriented east and south-east in the area of study. Therefore, around 35% of tornadoes formed over the sea that hit land move from SE to NW and 30% from SSE to NNW. The orientation of damage paths is related to the typical synoptic pattern under which tornadic activity occurs in the region of study, which is usually characterised by southerly mid- and upper-level winds due to a deep through or a low located west from Catalonia (e.g., Aran et al., 2009; Bech et al., 2011, 2015).

3.5. Socioeconomic impact

Between 2000 and 2019 no fatalities due to tornadoes were registered in the region of study. The last deathly tornadic event reported was on 27 November 1930 between Tarragona and la Selva del Camp (Gay`a, 2018). Nevertheless, at least 26 people have been injured during the period of study (Table 3). Most of them (22) were associated to urban events, where the population density is high, a factor which is positively correlated to casualties (Donner, 2007). The rest (4), were located in campings, where constructions (mobile homes, vans, bungalows) are more vulnerable than in urban areas, as it is indicated in Eidson et al. (1990). The most common injury types were bruises, cuts and fractures, similar than reported in other studies (e.g., Brown et al., 2002).

All these injuries have been caused by 6 individual tornadoes (around 6% of the total), which in general have been rated as EF1+. Only one person was injured by an EF0 tornado, during the 7 and 8 September 2005 outbreak (Bech et al., 2007). Moreover, a vast majority of injuring events (4) occurred during daytime hours (between 06 and 18 UTC). From the present dataset it stands out the case of the 18 October 2017 tornado that hit Valls, a 24,000 inhabitants town located 20 km north of Tarragona, which caused 13 people injured.

The annual number of injured people is highly irregular, being a typical pattern of rare events (Table 3). This is because injuring tornadoes are usually restricted to the occurrence of two simultaneous conditions which do not concur every year, as previously pointed out: (i) the tornado intensity is normally greater than EF0 (it corresponds to 28% of all reported events), and (ii) the tornado generally hits urban areas.

Damage loss estimation also presents a large interannual variability (Fig. 12). This behaviour, which is observed in other tornado datasets (Antonescu et al., 2017; NOAA/SPC, 2019) and other natural disasters (e.g., Barredo et al., 2012), obviously depends on the characteristics of each event and the affected area (Romanic et al., 2016). Here, great damage losses are usually related to EF1+ events hitting high-densely populated areas or important infrastructures (see for example year 2006, when an EF1 tornado affected several towns close to Barcelona; Mateo et al., 2009).

Between 2004 and 2019, the CCS paid 20.0 M€ on reinsurance

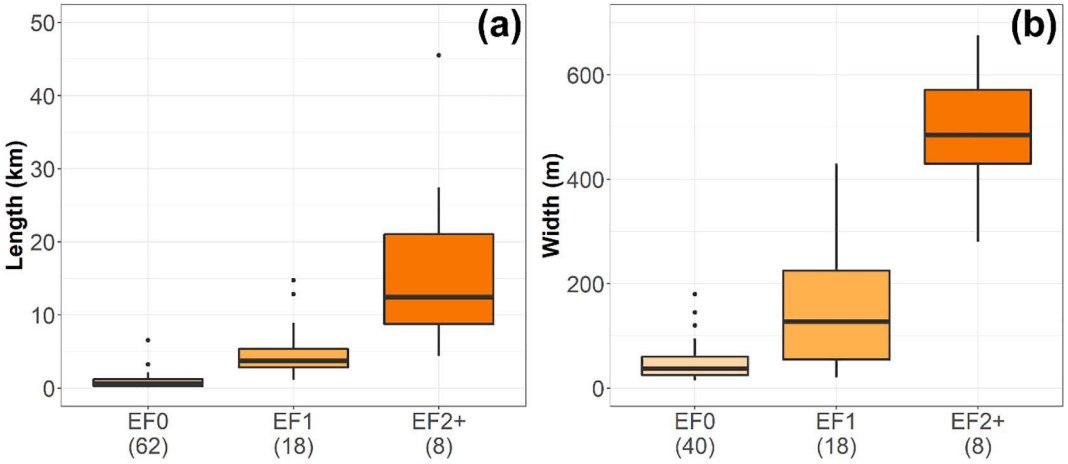

Fig. 10. Boxplots showing the track length (a) and width (b) for tornadoes reported in Catalonia depending on the EF-scale. It is represented 25th, 50th, and 75th percentiles and outlier points (exceeding the distance to the 25th or 75th percentile by 1.5 times the inter-quartile range). In brackets it is shown the number of paths for each EF category.

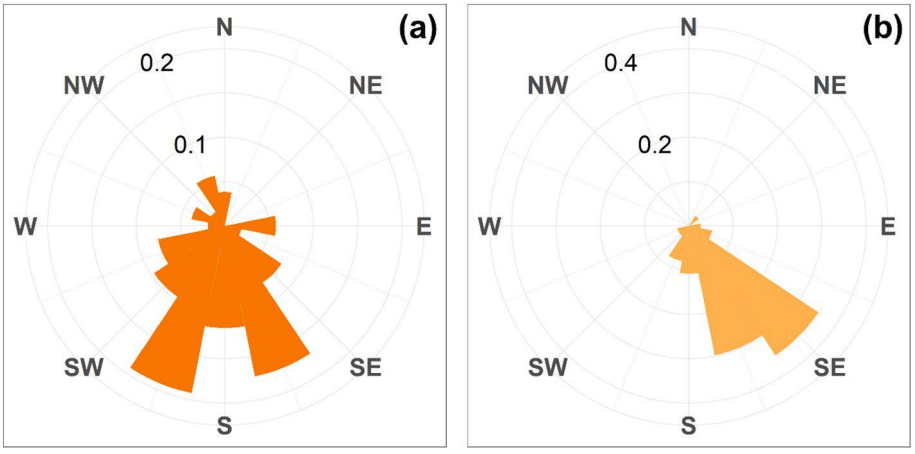

Fig. 11. Relative frequency of tornado path directions for inland (a) and offshore (b) touchdown cases.

Table 3
List of tornados and their intensity according to the EF-scale causing injuries during 2000–2019.

Date	EF	Injuries	Reference
7 September 2005	1	2	Bech et al. (2007)
7 September 2005	0	1	Bech et al. (2007)
13 September 2006	1	3	Mateo et al. (2009)
2 November 2008	2	4	Bech et al. (2011)
18 October 2017	1	13	Bech et al. (2018)
22 October 2019	2	3	–

compensations for tornado-related damage on insured properties (updated on 31 December 2019; light-grey columns in Fig. 12), although the real cost of repairing the covered damage is estimated on 22.5 M€ (dark-grey columns in Fig. 12). Nevertheless, taking into account data from local administration and expert assessment, the sum of the global damage loss estimation during the analysed 20-years period rises up to 30.8 M€ (red columns in Fig. 12). This figure, which implies an average of 1.5 M€ per year, is one magnitude order smaller than CCS floods compensations paid in Catalonia between 1996 and 2015 (21.8 M€ per year; Cort`es et al., 2018).

The difference between CCS paid amounts and the global cost estimation is greater for rural tornadoes than for urban events. This might be caused by a lack of insurances covering part of rural buildings such as farms and warehouses. On those cases, the Public Reinsurance Company does not compensate damage. This situation is illustrated by a case in 2018, when a long-track tornado affected a rural area in northern Catalonia (Rodríguez et al., 2018). Local administration estimated damage losses on 4.3 M€, whereas CCS only covered 0.7 M€ (16%).

On years when at least one significant tornado is reported, the damage loss estimation surpasses 1 M€ (Fig. 6a and red columns in Fig. 12). Ten individual events produced estimated damage higher than 1 M€. From those, two caused damage greater than 5 M€ (13 September 2006 EF1 tornado 18 km SW Barcelona, and 2 November 2008 EF2 tornado 12 km SW Tarragona). In contrast, no EF0 event caused estimated losses greater than 0.5 M€.

4. Conclusions and final remarks

In this article, tornado and waterspout events reported in Catalonia (NE Iberian Peninsula) between 2000 and 2019 have been analysed. During the second half of the period of study, social networks were the main source of severe weather information, enlarging the number of waterspouts (especially formed far-away from the coast) and EF0 tornadoes (mainly in lower densely-populated areas) reports. A total of 105 tornadoes (41 of them formed offshore) and 329 waterspouts have been observed during this 20-years period, which yields yearly averages of 5.3 tornadoes year^{-1} and 16.5 waterspout year^{-1} respectively. Areal and linear density over the region and the coast are, respectively, 1.65

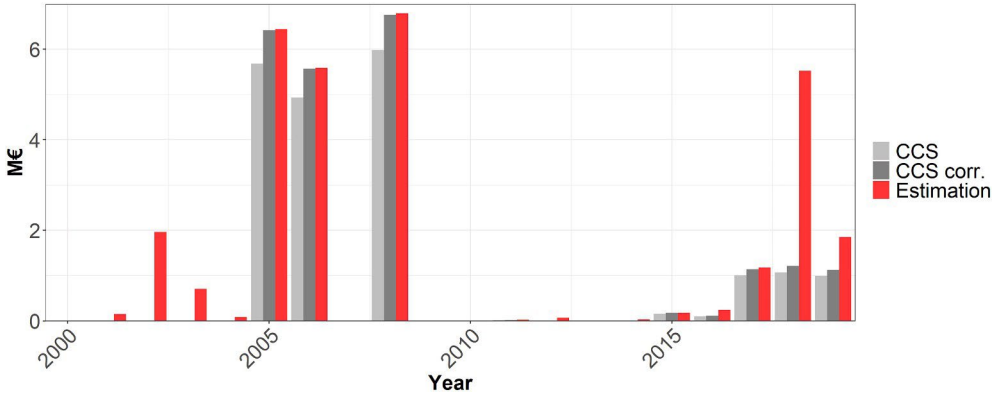

Fig. 12. Yearly tornadic events costs: CCS compensations, corrected (+13%) CCS compensations, and total damage-loss estimations (in Million Euros homogenized to 31 December 2019).

tornadoes year^{-1} 10^{-4} km^{-2} and 5.0 waterspouts year^{-1} 10^{-2} km^{-1}, slightly higher than in other Mediterranean countries.

Most tornadoes and waterspouts have been detected in the central sector of the littoral and pre-littoral, coinciding with the most populated area of the region. Nevertheless, meteorological and geographical factors such as the formation of mesoscale convergence lines in northerly situations due to the orographic effect of the Pyrenees, and the combination of increasing wind-shear environments during late summer and autumn with the period of highest instability due to high sea surface temperature might provide favourable conditions for tornado formation in this zone. In fact, 69% tornadoes and 75% waterspouts have been reported between August and November, similarly with previous studies. Moreover, tornadoes have usually occurred between 15 and 18 UTC, being related to deep-moist convection supported by the solar diurnal heating cycle. In contrast, waterspouts have been mainly observed during the morning (06–12 UTC) and late afternoon (15–18 UTC), presenting a secondary minimum during early afternoon, which is consistent with lightning climatology in the Balearic sea. Nevertheless, lightning activity over the western Mediterranean is maximum between 18 and 06 UTC, which would suggest that nocturnal waterspouts are much more underreported than nocturnal tornadic events.

During the period of study, 17 tornado outbreaks were identified, two of them qualified as moderate (between 11 and 20 vortices formed within the same synoptic system) and one, as large (more than 20 vortices). Moreover, 158 tornadoes and waterspouts were associated with 54 multiple events. The observation of five or more independent vortices in this kind of events is rare, representing 6% of the total, whereas the most common reported multiple events are those with only two independent vortices (52%).

Most tornadoes (92%) observed in Catalonia were weak (EF0/EF1), and only 8% were significant (EF2+). The strongest tornado took place 30 km north of Tarragona on 2 November 2008 and reached EF3 intensity. Most damage paths have been less than 5 km long (82%) and 200 m wide (79%), and a positive correlation between tornado strength and damage swath size has been observed. The tornado tracks studied presented a direction usually ranging from SE-NW to SW-NE, being the SE-NW direction the predominant for waterspouts that make landfall, due to the coast orientation.

Only 6 of the reported tornado events, mostly EF1+, caused injuries. In total, 26 people were injured, mainly with bruises, cuts and fractures, and no fatalities were registered. The damage loss estimation raised up to 30.8 M€, with a median of 1.5 M€ per year, which is one magnitude order smaller than floods compensations payed by the reinsurance public company of Spain in the area of study.

The analysis performed here may contribute to deepen in the knowledge of tornado and waterspouts frequency and characteristics in this hotspot area of the western Mediterranean. Moreover, the data provided in the appendix is available for the scientific community, and may be useful to validate and test nowcasting products and develop new studies to enhance tornadic storms forecasting and surveillance systems.

Future work could also include a more detailed weather radar analysis to objectively identify radar signatures supporting convective storm organization, allowing to distinguish supercell vs. non-supercell tornado features. Further studies could also expand the analysis of outbreaks to the rest of the Mediterranean slope of the Iberian Peninsula, Balearic Islands, southern France and even NW of Italy. Finally, a larger database including more years could also attempt to study possible temporal trends in the data set.

Declaration of Competing Interest

The authors declare that they have no known competing financial interests or personal relationships that could have appeared to influence the work reported in this paper.

Acknowledgments

We thank weather spotters, casual witnesses, meteorologists from the Meteorological Service of Catalonia and the Spanish Meteorological Agency, and weather presenters from Catalan media for reporting us tornado and waterspout events. We also appreciate the fire-fighters of the Government of Catalonia and Local Administration for providing tornado-related incidents, and the *Consorcio de Compensacio´n de Seguros* (CCS) for providing data about tornado damage compensations. This study has been carried out into the framework of the HyMeX (HYdrological cycle in the Mediterranean EXperiment) international research programme and with partial support from projects CGL2015-65627-C3-2-R (MINECO/FEDER), CGL2016-81828-REDT (AEI) and RTI2018-098693-B-C32 (AEI), and the Water Research Institute (IdRA) of the University of Barcelona.

Appendix A

Here, it is provided a list of individual tornado and waterspout events analysed in the present article for open use in further research (see Table A1).

Table A1
Individual tornado and waterspouts analysed in this study including for each item listed the number (#), UTC Date and Time (in YYYY/MM/DD HH:mm format), Latitude (°), Longitude (°) and Enhanced Fujita intensity (EF) for tornadoes or W for waterspouts. In five waterspout cases, time was not available.

Item (#)	Date & Time (UTC)	Lat (°)	Lon (°)	EF/W (n/W)
001	2000/06/11 17:00	41.245	2.060	W
002	2000/12/21 13:30	41.497	2.576	W
003	2000/12/23 06:50	42.338	3.040	0
004	2000/12/23 11:55	41.570	2.566	W
005	2001/04/19 08:32	41.698	2.848	0
006	2001/04/27 16:00	42.000	2.284	0
007	2001/08/31 14:30	41.223	1.934	W
008	2001/08/31 14:30	41.219	1.948	W
009	2001/08/31 14:30	41.210	1.971	W
010	2001/10/20 03:00	41.659	2.405	1
011	2001/10/20 03:15	42.033	2.455	1
012	2001/10/20 03:45	42.247	2.883	1
013	2001/10/20 04:00	42.344	3.064	0
014	2001/10/20 10:15	41.621	2.692	0
015	2001/10/20 13:50	41.735	3.133	W
016	2001/11/09 07:30	41.308	2.724	W
017	2001/11/16 08:15	41.454	2.297	W
018	2002/06/05 16:30	41.632	2.858	W
019	2002/08/03 –:–	41.139	1.554	W
020	2002/08/08 16:35	41.701	2.994	W
021	2002/08/27 –:–	41.510	2.476	W
022	2002/09/16 07:00	40.614	0.911	W
023	2002/09/16 07:00	40.629	0.939	W
024	2002/10/10 07:30	41.363	2.299	W
025	2002/10/10 15:45	41.125	1.759	W
026	2002/10/21 15:48	41.641	0.605	1
027	2002/10/21 16:15	42.009	1.392	2
028	2002/11/15 16:30	41.428	2.422	W
029	2002/11/20 09:41	41.483	2.337	0
030	2003/08/17 07:30	41.280	1.246	0
031	2003/08/17 08:30	41.708	1.845	1
032	2003/08/17 09:00	41.788	2.226	1
033	2003/08/17 09:02	41.359	2.219	W
034	2003/08/17 –:–	41.501	2.489	W
035	2003/08/23 01:10	41.186	1.569	0
036	2003/09/04 17:00	40.988	0.931	W
037	2003/09/22 06:45	41.765	3.087	W
038	2003/09/22 06:45	41.758	3.083	W
039	2003/10/01 01:45	41.128	1.137	0
040	2004/07/05 15:45	41.472	0.443	1
041	2004/07/10 09:49	40.999	1.126	W
042	2004/08/05 00:20	41.265	1.997	0
043	2004/08/05 01:45	41.137	1.647	W
044	2004/08/10 12:00	41.130	1.495	W
045	2004/08/29 13:30	41.021	1.299	W
046	2004/08/30 06:24	40.990	1.026	W
047	2004/08/30 06:29	40.987	1.052	W
048	2004/09/20 11:00	41.382	2.213	W
049	2004/10/18 11:00	41.011	1.483	W
050	2004/10/30 18:00	42.028	3.228	W
051	2004/11/01 16:00	41.218	1.934	W
052	2004/11/10 18:30	40.998	2.202	W
053	2004/11/22 13:30	41.147	1.640	W
054	2004/12/01 20:45	41.147	1.422	1
055	2004/12/01 21:00	41.216	1.740	0
056	2005/01/29 16:30	41.132	1.753	W
057	2005/08/02 18:00	41.104	1.548	W
058	2005/09/07 17:05	41.261	1.932	1
059	2005/09/07 17:15	41.264	1.995	0
060	2005/09/07 17:23	41.228	2.162	W
061	2005/09/07 17:29	41.280	2.086	2
062	2005/09/07 17:30	41.533	2.637	W
063	2005/09/07 17:30	41.540	2.648	W
064	2005/09/07 17:39	41.210	2.256	W
065	2005/09/07 17:48	41.292	2.117	1
066	2005/09/07 17:52	41.239	2.234	W
067	2005/09/07 17:52	41.229	2.266	W
068	2005/09/07 18:00	41.534	2.511	W
069	2005/09/07 18:10	41.595	2.716	W
070	2005/09/07 18:18	41.315	2.114	0
071	2005/09/07 20:00	41.593	2.602	0

(*continued on next page*)

Table A1 (*continued*)

Item (#)	Date & Time (UTC)	Lat (°)	Lon (°)	EF/W (n/W)
072	2005/09/08 05:00	41.164	1.889	W
073	2005/09/08 05:45	40.896	0.834	W
074	2005/09/08 07:30	41.506	2.208	1
075	2005/09/08 12:40	41.028	1.872	W
076	2005/09/08 13:00	41.172	1.821	W
077	2005/09/08 14:00	41.119	1.755	W
078	2005/09/08 15:30	41.044	1.297	W
079	2005/10/05 08:10	41.399	2.362	W
080	2005/10/13 07:00	41.780	3.033	0
081	2005/10/13 12:40	41.214	1.820	W
082	2005/10/14 11:15	41.289	2.205	W
083	2005/10/15 14:00	41.243	1.980	W
084	2005/10/15 15:45	41.468	2.297	W
085	2005/11/13 13:28	41.139	1.622	W
086	2005/11/13 16:40	41.126	1.539	W
087	2005/11/14 16:45	40.830	1.835	W
088	2005/11/14 20:15	41.636	2.730	0
089	2005/11/14 20:15	41.663	2.784	0
090	2005/11/15 08:58	41.239	1.976	W
091	2005/11/15 08:58	41.212	2.128	W
092	2005/11/15 14:50	41.724	0.837	0
093	2005/11/15 14:50	40.853	1.040	W
094	2006/02/19 08:45	41.102	1.495	W
095	2006/02/21 15:30	41.190	2.692	W
096	2006/02/21 16:15	41.230	2.021	W
097	2006/02/21 16:15	41.215	2.006	W
098	2006/02/21 16:15	41.223	2.014	W
099	2006/02/21 17:00	41.230	2.028	W
100	2006/08/10 18:30	41.526	2.634	W
101	2006/08/11 14:00	41.340	2.164	0
102	2006/08/14 09:19	40.686	2.518	W
103	2006/08/15 15:45	41.151	1.663	W
104	2006/08/16 06:00	40.532	0.845	W
105	2006/08/16 15:30	41.056	1.062	W
106	2006/08/16 15:55	41.095	1.320	W
107	2006/08/16 17:00	41.168	1.488	0
108	2006/09/12 07:30	41.444	2.690	W
109	2006/09/13 08:20	41.169	1.743	W
110	2006/09/13 08:50	41.589	2.592	0
111	2006/09/13 09:00	41.052	1.516	W
112	2006/09/13 09:05	41.097	1.514	W
113	2006/09/13 09:15	41.134	1.402	1
114	2006/09/13 09:30	41.196	1.497	0
115	2006/09/13 10:28	41.242	1.876	W
116	2006/09/13 10:30	41.260	1.945	W
117	2006/09/13 10:30	41.260	1.948	W
118	2006/09/13 10:30	41.229	1.971	W
119	2006/09/13 10:49	41.267	2.029	1
120	2006/09/18 09:46	41.356	2.349	W
121	2006/09/18 10:45	41.463	2.436	W
122	2006/09/18 10:45	41.456	2.469	W
123	2006/09/18 11:00	41.561	2.642	W
124	2006/09/18 11:00	41.556	2.630	W
125	2006/10/11 08:30	41.192	1.754	W
126	2006/10/11 08:30	41.182	1.734	W
127	2006/10/14 –:–	41.738	3.083	W
128	2006/10/14 –:–	40.961	0.981	W
129	2006/10/18 13:21	41.729	2.141	2
130	2007/05/01 08:00	41.202	1.723	W
131	2007/05/01 14:04	41.483	2.644	W
132	2007/05/01 14:45	41.790	3.167	W
133	2007/06/18 15:45	41.236	1.995	W
134	2007/08/12 20:00	41.232	1.864	W
135	2007/08/12 21:30	41.574	2.542	0
136	2007/08/19 10:05	41.164	1.491	W
137	2007/08/21 17:40	41.345	2.035	0
138	2007/08/22 07:30	41.206	1.870	W
139	2007/08/22 07:30	41.212	1.892	W
140	2007/08/24 11:45	40.506	0.676	W
141	2007/08/24 11:45	40.501	0.660	W
142	2007/08/24 12:00	40.933	1.395	W
143	2007/09/27 20:00	41.402	2.315	W
144	2007/10/05 04:00	41.271	1.986	0
145	2007/10/08 09:48	41.484	2.563	W
146	2007/10/10 19:50	41.092	1.949	W

(*continued on next page*)

Table A1 (*continued*)

Item (#)	Date & Time (UTC)	Lat (°)	Lon (°)	EF/W (n/W)
147	2008/03/04 12:30	41.957	2.632	0
148	2008/03/09 16:45	41.137	1.502	W
149	2008/03/09 16:45	41.135	1.494	W
150	2008/03/09 16:45	41.131	1.485	W
151	2008/04/17 15:27	41.469	2.189	0
152	2008/05/10 18:42	40.648	0.615	0
153	2008/05/11 06:20	40.749	0.937	W
154	2008/05/17 09:47	41.723	1.550	0
155	2008/05/19 15:05	41.218	1.840	W
156	2008/06/17 12:15	41.397	1.798	0
157	2008/07/12 15:50	41.044	1.248	W
158	2008/08/25 18:45	41.131	1.367	0
159	2008/09/13 18:00	41.233	2.508	W
160	2008/09/13 18:00	41.246	2.523	W
161	2008/09/13 18:00	41.252	2.485	W
162	2008/09/25 07:30	41.295	2.633	W
163	2008/09/26 10:45	41.076	1.976	W
164	2008/10/17 16:45	41.249	1.903	W
165	2008/11/01 01:45	41.686	2.816	0
166	2008/11/02 02:59	41.074	1.122	2
167	2008/11/02 03:32	41.375	1.315	3
168	2008/11/06 13:15	41.506	2.626	W
169	2009/04/01 16:30	41.127	1.727	W
170	2009/04/10 13:55	41.664	2.785	0
171	2009/04/11 14:15	41.090	1.347	W
172	2009/04/11 15:27	41.307	2.341	W
173	2009/08/09 12:30	41.397	2.237	W
174	2009/08/09 15:05	42.227	1.734	1
175	2009/08/25 15:45	41.604	0.419	0
176	2009/09/14 15:28	41.397	2.262	W
177	2009/09/14 17:04	41.257	2.072	W
178	2009/09/30 06:00	41.225	1.858	W
179	2009/09/30 06:00	41.181	2.043	W
180	2009/10/09 06:30	40.809	1.174	W
181	2009/10/09 06:30	40.817	1.177	W
182	2009/10/21 03:35	41.131	1.369	0
183	2010/04/04 15:35	41.626	2.238	0
184	2010/07/23 19:10	41.252	1.983	W
185	2010/08/12 19:00	41.138	1.472	W
186	2010/08/19 16:30	40.511	0.578	W
187	2010/09/20 07:10	41.277	2.132	W
188	2010/09/21 08:15	41.366	2.316	W
189	2010/09/26 18:00	41.461	2.326	W
190	2010/10/11 14:25	41.265	1.583	0
191	2010/10/11 15:00	41.612	1.242	0
192	2010/10/11 15:25	41.284	2.369	W
193	2010/10/11 15:45	41.232	2.030	W
194	2010/10/11 15:48	41.011	2.144	W
195	2010/10/11 16:06	41.013	1.948	W
196	2010/10/11 16:36	41.115	1.618	W
197	2010/10/11 16:54	41.061	1.502	W
198	2010/10/11 17:15	41.198	1.996	W
199	2011/04/24 09:00	40.608	0.827	W
200	2011/06/01 17:40	41.289	2.150	W
201	2011/07/12 21:50	41.134	1.380	0
202	2011/09/03 21:10	41.306	2.170	W
203	2011/09/24 05:30	41.264	1.964	0
204	2011/10/22 15:35	41.846	3.108	0
205	2011/10/22 16:34	41.839	3.125	W
206	2011/10/23 12:30	41.443	2.415	W
207	2011/11/02 15:00	41.053	1.099	W
208	2011/11/05 15:00	41.060	1.577	W
209	2011/11/05 15:00	41.053	1.563	W
210	2011/11/05 15:00	41.049	1.550	W
211	2011/11/05 15:30	41.094	1.546	W
212	2011/11/05 15:30	41.096	1.541	W
213	2011/11/05 15:30	41.100	1.533	W
214	2011/11/06 14:25	41.832	3.119	W
215	2011/12/27 14:34	41.441	2.857	W
216	2012/03/21 18:45	41.657	0.996	1
217	2012/04/06 08:00	40.983	0.923	W
218	2012/04/14 15:30	42.027	3.138	0
219	2012/04/19 15:10	41.912	3.213	W
220	2012/05/20 09:45	42.137	2.436	0
221	2012/09/02 00:00	41.216	1.830	W

(*continued on next page*)

Table A1 (*continued*)

Item (#)	Date & Time (UTC)	Lat (°)	Lon (°)	EF/W (n/W)
222	2012/10/12 17:40	41.134	1.409	W
223	2012/10/13 08:30	41.086	1.872	W
224	2012/10/21 12:54	41.031	1.129	W
225	2012/10/21 16:45	41.359	2.440	W
226	2012/10/27 16:45	41.440	2.262	W
227	2012/10/27 16:51	41.381	2.229	W
228	2012/10/27 16:55	41.307	2.168	W
229	2013/06/08 13:55	41.362	1.293	0
230	2013/06/18 13:35	41.320	0.875	0
231	2013/07/16 14:15	41.726	1.449	0
232	2013/08/08 00:49	41.294	2.431	W
233	2013/08/17 11:15	41.021	1.667	W
234	2013/08/28 14:20	41.180	1.609	W
235	2013/09/07 11:15	41.011	1.342	W
236	2013/09/10 21:06	41.287	2.139	W
237	2013/09/10 21:07	41.274	2.182	W
238	2013/09/10 21:24	41.248	2.259	W
239	2013/09/30 10:30	41.597	3.327	W
240	2013/10/06 15:05	41.384	2.359	W
241	2013/10/06 15:56	41.213	2.319	W
242	2013/10/07 06:10	40.390	1.538	W
243	2013/10/10 17:00	41.418	3.213	W
244	2013/10/19 10:15	41.037	1.513	W
245	2013/10/19 10:15	40.898	1.456	W
246	2013/11/17 10:55	41.236	2.038	W
247	2013/11/17 14:00	41.176	1.695	W
248	2014/05/30 16:36	41.253	1.321	0
249	2014/06/25 06:45	41.712	3.242	W
250	2014/07/29 14:30	41.246	2.181	W
251	2014/09/04 09:30	40.994	1.059	W
252	2014/09/05 19:05	41.560	2.267	0
253	2014/09/14 10:08	40.947	0.977	W
254	2014/09/14 10:15	40.971	0.894	0
255	2014/09/16 05:30	40.469	0.740	W
256	2014/09/16 23:40	41.387	2.274	W
257	2014/09/18 07:30	-	-	W
258	2014/09/23 12:55	42.065	2.311	0
259	2014/11/03 14:37	41.641	2.760	W
260	2014/11/26 08:45	41.115	1.550	W
261	2014/11/28 01:10	41.113	1.229	0
262	2014/12/06 13:54	41.448	2.696	W
263	2014/12/09 03:50	40.702	2.869	W
264	2014/12/09 03:50	40.697	2.849	W
265	2014/12/09 03:51	40.731	2.796	W
266	2015/01/31 23:37	41.459	3.440	W
267	2015/01/31 23:38	41.459	3.481	W
268	2015/02/01 00:17	41.308	3.657	W
269	2015/02/01 00:51	41.082	3.995	W
270	2015/06/13 18:10	41.078	1.305	W
271	2015/08/13 16:30	41.349	2.379	W
272	2015/08/15 14:44	41.553	2.664	W
273	2015/08/16 05:15	40.601	1.707	W
274	2015/09/06 22:30	41.243	2.049	W
275	2015/09/10 11:30	41.153	1.525	W
276	2015/09/11 09:00	40.931	1.094	W
277	2015/10/09 07:10	40.635	1.254	W
278	2015/11/02 15:28	41.022	0.959	1
279	2015/11/02 18:00	41.387	1.186	0
280	2016/02/27 04:30	41.234	1.807	0
281	2016/02/27 05:10	41.611	2.658	0
282	2016/02/27 17:45	41.315	2.194	W
283	2016/03/07 02:38	41.286	2.900	W
284	2016/03/21 15:45	41.456	1.814	0
285	2016/06/16 18:40	41.947	3.239	W
286	2016/08/09 21:30	40.710	1.100	W
287	2016/08/09 21:30	40.699	1.072	W
288	2016/09/08 10:45	40.584	1.242	W
289	2016/09/10 01:00	41.615	2.673	0
290	2016/09/10 06:30	40.545	0.871	W
291	2016/09/10 06:33	40.532	0.865	W
292	2016/09/10 06:45	40.525	0.867	W
293	2016/09/14 08:15	41.999	3.270	W
294	2016/09/15 18:03	41.564	3.175	W
295	2016/09/21 05:25	41.481	2.418	W
296	2016/09/23 06:45	40.551	0.782	W

(*continued on next page*)

Table A1 (*continued*)

Item (#)	Date & Time (UTC)	Lat (°)	Lon (°)	EF/W (n/W)
297	2016/09/24 09:00	41.725	3.111	W
298	2016/10/02 08:15	41.255	2.103	W
299	2016/10/03 09:45	40.921	1.358	W
300	2016/10/13 08:00	40.960	1.121	W
301	2016/10/13 08:00	40.945	1.142	W
302	2016/10/13 09:15	41.096	1.751	W
303	2016/10/13 12:00	41.037	1.435	W
304	2016/10/13 15:30	41.638	2.414	1
305	2016/10/13 16:58	41.118	0.746	0
306	2016/10/14 16:45	41.681	2.943	W
307	2016/10/14 16:45	41.680	2.934	W
308	2016/10/14 16:50	41.754	3.083	W
309	2016/10/14 16:50	41.755	3.077	W
310	2016/11/05 17:06	42.022	1.997	1
311	2016/11/07 10:00	41.185	2.361	W
312	2016/11/07 10:00	41.220	2.408	W
313	2016/11/07 10:00	41.218	2.422	W
314	2016/11/23 14:30	41.171	1.659	W
315	2016/11/23 16:12	41.522	2.428	0
316	2016/11/26 08:15	41.245	2.112	W
317	2016/11/26 09:15	41.259	2.275	W
318	2016/11/26 15:09	41.143	1.931	W
319	2016/11/26 16:10	41.098	1.793	W
320	2016/11/26 16:21	41.110	1.766	W
321	2016/11/26 16:32	41.110	1.783	W
322	2016/11/26 16:42	41.138	1.743	W
323	2016/11/26 17:18	41.196	1.681	W
324	2016/11/27 11:03	41.212	1.981	W
325	2016/11/27 11:04	41.196	1.723	W
326	2016/12/04 13:51	40.747	0.661	0
327	2017/01/25 15:55	41.120	1.394	W
328	2017/03/24 10:59	40.749	1.104	W
329	2017/03/24 11:06	40.755	1.116	W
330	2017/03/24 11:15	40.727	1.126	W
331	2017/06/29 10:10	41.821	3.258	W
332	2017/08/10 21:06	41.367	2.425	W
333	2017/09/16 07:43	41.447	2.779	W
334	2017/09/16 21:51	41.135	2.226	W
335	2017/09/22 09:00	41.288	2.284	W
336	2017/10/18 16:00	41.263	1.246	1
337	2017/11/04 10:15	40.944	0.918	W
338	2017/11/04 16:30	41.155	1.457	W
339	2017/12/01 13:25	41.554	0.809	0
340	2017/12/01 16:05	40.985	1.760	W
341	2017/12/01 16:05	41.028	1.786	W
342	2017/12/01 16:25	40.956	1.813	W
343	2017/12/01 16:25	40.951	1.800	W
344	2017/12/01 16:50	41.046	1.807	W
345	2017/12/01 16:50	41.054	1.817	W
346	2017/12/12 15:30	41.085	2.504	W
347	2018/01/07 00:53	41.903	1.702	2
348	2018/01/07 07:22	42.209	2.858	2
349	2018/01/07 09:00	41.581	2.210	0
350	2018/02/04 14:40	40.995	0.929	0
351	2018/02/05 07:30	41.218	1.828	W
352	2018/02/08 16:10	41.103	1.524	W
353	2018/02/12 15:52	41.109	1.320	W
354	2018/03/07 06:13	41.227	2.927	W
355	2018/03/07 06:13	41.206	2.919	W
356	2018/03/07 06:13	41.172	2.901	W
357	2018/03/07 06:22	41.170	2.967	W
358	2018/03/07 06:25	41.121	3.032	W
359	2018/03/07 06:25	41.031	3.046	W
360	2018/03/07 06:35	41.039	3.137	W
361	2018/03/07 06:35	40.956	3.112	W
362	2018/03/13 08:20	41.585	2.604	W
363	2018/04/13 08:30	41.097	1.160	0
364	2018/05/28 10:35	40.707	0.714	0
365	2018/05/29 04:55	41.512	2.451	W
366	2018/06/06 11:40	41.505	2.610	W
367	2018/06/06 11:40	41.485	2.626	W
368	2018/06/06 13:20	41.758	3.150	W
369	2018/06/06 13:20	41.755	3.141	W
370	2018/06/07 09:27	41.564	3.490	W
371	2018/07/16 06:55	41.383	2.205	W

(*continued on next page*)

Table A1 (*continued*)

Item (#)	Date & Time (UTC)	Lat (°)	Lon (°)	EF/W (n/W)
372	2018/07/16 07:00	41.369	2.180	W
373	2018/08/08 09:00	40.753	1.003	W
374	2018/08/12 18:30	41.153	1.552	W
375	2018/08/17 08:30	40.982	2.261	W
376	2018/08/17 08:30	40.963	2.232	W
377	2018/08/17 08:30	40.950	2.214	W
378	2018/08/17 12:40	41.465	2.340	W
379	2018/08/17 13:45	41.188	1.577	0
380	2018/09/01 17:20	41.186	1.500	0
381	2018/10/08 16:56	41.424	2.281	W
382	2018/10/09 05:47	41.242	2.314	W
383	2018/10/09 05:50	41.181	2.351	W
384	2018/10/09 05:53	41.213	2.385	W
385	2018/10/09 07:28	41.326	2.177	W
386	2018/10/09 09:48	41.249	1.908	W
387	2018/10/09 22:39	41.860	2.659	0
388	2018/10/10 11:17	40.793	0.962	W
389	2018/10/10 11:27	40.823	0.969	W
390	2018/10/10 11:34	40.866	1.010	W
391	2018/10/10 12:01	40.920	1.125	W
392	2018/10/14 19:55	41.165	1.260	1
393	2018/10/14 23:30	41.180	1.253	0
394	2018/10/15 01:39	41.636	2.729	1
395	2018/11/15 07:07	41.571	1.982	0
396	2018/11/15 09:40	41.326	2.202	W
397	2019/04/07 13:45	41.585	2.659	W
398	2019/04/07 13:47	41.576	2.671	W
399	2019/04/07 13:47	41.568	2.672	W
400	2019/04/24 06:56	41.255	2.322	W
401	2019/08/15 22:16	41.381	2.194	0
402	2019/08/27 10:05	41.288	2.232	W
403	2019/08/27 11:54	41.208	1.716	W
404	2019/08/27 12:32	41.051	1.173	W
405	2019/08/27 12:35	41.089	1.215	W
406	2019/08/27 13:05	40.767	0.851	W
407	2019/09/07 11:15	41.105	1.844	W
408	2019/09/08 08:24	41.229	2.239	W
409	2019/09/08 11:28	41.093	2.149	W
410	2019/09/08 14:35	41.280	2.084	0
411	2019/09/08 14:40	41.312	2.091	0
412	2019/09/08 15:47	41.342	2.150	0
413	2019/09/08 16:15	41.331	2.161	0
414	2019/09/08 16:45	41.299	2.164	W
415	2019/09/09 21:59	41.367	2.407	W
416	2019/09/09 22:03	41.316	2.339	W
417	2019/09/09 22:18	41.409	2.463	W
418	2019/09/09 22:43	41.321	2.410	W
419	2019/09/10 08:30	40.756	1.530	W
420	2019/09/10 08:30	40.748	1.516	W
421	2019/09/10 15:45	41.107	0.675	0
422	2019/09/28 07:00	40.994	1.592	W
423	2019/10/16 06:00	42.387	3.376	W
424	2019/10/20 03:35	41.465	2.280	0
425	2019/10/21 08:45	41.332	2.349	W
426	2019/10/21 09:37	41.353	2.407	W
427	2019/10/22 13:47	40.982	0.994	W
428	2019/10/22 23:53	41.710	2.533	2
429	2019/10/23 11:22	41.240	1.995	W
430	2019/10/23 11:59	41.260	2.010	W
431	2019/10/23 13:45	41.833	3.173	W
432	2019/10/23 16:39	41.195	1.830	W
433	2019/11/08 02:32	41.222	3.052	W
434	2019/11/14 14:05	41.473	2.485	W

References

Altube, P., Bech, J., Argemí, O., Rigo, T., 2015. Quality control of Antenna alignment and receiver calibration using the sun: Adaptation to Midrange Weather Radar observations at low elevation angles. J. Atmos. Ocean. Technol. 32, 927–942. https://doi.org/10.1175/JTECH-D-14-00116.1.

Altube, P., Bech, J., Argemí, O., Rigo, T., Pineda, N., Collis, S., Helmus, J., 2017. Correction of dual-PRF Doppler velocity outliers in the presence of aliasing. J. Atmos. Ocean. Technol. 34 (7), 1529–1543. https://doi.org/10.1175/JTECH-D-16-0065.1.

AMS, 2020. Glossary of Meteorology. American Meteorological Society. http://glossary.ametsoc.org (last access 4 November 2020).

Antonescu, B., Schultz, D.M., Lomas, F., Kühne, T., 2016. Tornadoes in Europe: synthesis of the observational datasets. Mon. Weather Rev. 144, 2445–2480. https://doi.org/10.1175/MWR-D-15-0298.1.

Antonescu, B., Schultz, D.M., Holzer, A., Groenemeijer, P., 2017. Tornadoes in Europe: an underestimated threat. Bull. Am. Meteorol. Soc. 98, 713–728. https://doi.org/10.1175/BAMS-D-16-0171.1.

Antonescu, B., Ricketts, H.M., Schultz, D.M., 2019. 100 years later: reflecting on Alfred Wegener's contributions to Tornado research in Europe. Bull. Am. Meteorol. Soc. 100, 567–578. https://doi.org/10.1175/BAMS-D-17-0316.1.

Antonescu, B., Pú˘cik, T., Schultz, D.M., 2020. Hindcasting the first Tornado forecast in Europe: 25 June 1967. Weather Forecast. 35, 417–436. https://doi.org/10.1175/WAF-D-19-0173.1.

Apsley, M.L., Mulder, K.J., Schultz, D.M., 2016. Reexamining the United Kingdom's Greatest Tornado outbreak: forecasting the limited extent of Tornadoes along a cold front. Weather Forecast. 31, 853–875. https://doi.org/10.1175/WAF-D-15-0131.1.

Aran, M., Amaro, J., Arús, J., Bech, J., Figuerola, F., Gaya`, M., Vilaclara, E., 2009. Synoptic and mesoscale diagnosis of a tornado event in Castellcir, Catalonia, on 18th October 2006. Atmos. Res. 93 (1–3), 147–160. https://doi.org/10.1016/j.atmosres.2008.09.031.

Barredo, J.L., Saurí, D., Llasat, M.C., 2012. Assessing trends in insured losses from floods in Spain 1971–2008. Nat. Hazards Earth Syst. Sci. 12, 1723–1729. https://doi.org/10.5194/nhess-12-1723-2012.

Bech, J., Pascual, R., Rigo, T., Pineda, N., Lo´pez, J.M., Arús, J., Gaya`, M., 2007. An observational study of the 7 September 2005 Barcelona tornado outbreak. Nat. Hazards Earth Syst. Sci. 7 (1), 129–139. https://doi.org/10.5194/nhess-7-129-2007.

Bech, J., Gaya`, M., Aran, M., Figuerola, F., Amaro, J., Arús, J., 2009. Tornado damage analysis of a forest area using site survey observations, radar data and a simple analytical vortex model. Atmos. Res. 93 (1–3), 118–130. https://doi.org/10.1016/j.atmosres.2008.10.016.

Bech, J., Pineda, N., Rigo, T., Aran, M., Amaro, J., Gaya`, M., Arús, J., Montanya`, J., van der Velde, O., 2011. A Mediterranean nocturnal heavy rainfall and tornadic event. Part I: Overview, damage survey and radar analysis. Atmos. Res. 100 (4), 621–637. https://doi.org/10.1016/j.atmosres.2010.12.024.

Bech, J., Arús, J., Cast´an, S., Pineda, N., Rigo, T., Montanya`, J., van der Velde, O., 2015. A study of the 21 March 2012 tornadic quasi linear convective system in Catalonia. Atmos. Res. 158–159, 192–209. https://doi.org/10.1016/j.atmosres.2014.08.009.

Bech, J., Rodríguez, O., Altube, P., Rigo, T., Pineda, N., Casta´n, S., Arús, J., Montany`a, J., 2018. Doppler radar observations of two tornadic thunderstorm cases in the Western Mediterranean region. In: 10th European Conference on Radar in Meteorology and Hydrology, p. 111. https://doi.org/10.18174/454537.

Brooks, H.E., 2004. On the relationship of tornado path length and width to intensity. Weather Forecast. 19, 310–319. https://doi.org/10.1175/1520-0434(2004)019<0310:OTROTP>2.0.CO;2.

Brooks, H.E., Lee, J.W., Craven, J.P., 2003. The spatial distribution of severe thunderstorm and tornado environments from global reanalysis data. Atmos. Res. 67–68, 73–94. https://doi.org/10.1016/S0169-8095(03)00045-0.

Brown, S., Archer, P., Kruger, E., Mallonee, S., 2002. Tornado-related deaths and injuries in Oklahoma due to the 3 May 1999 Tornadoes. Weather Forecast. 17, 343–353. https://doi.org/10.1175/1520-0434(2002)017<0343:TRDAII>2.0.CO;2.

Bunting, W.F., Smith, B.E., 1993. A guide for conducting damage surveys. In: NOAA Tech. Memo. NWS-SR-146, Scientific Services Division, Southern Region, Fort Worth, TX (44 pp).

Callado, A., Pascual, R., 2005. Diagnosis and modelling of a summer convective storm over Mediterranean Pyrenees. Adv. Geosci. 2, 273–277. https://doi.org/10.5194/adgeo-2-273-2005.

Calvo-Sancho, C., Martín, Y., 2020. The influence of synoptic weather patterns in supercell formation in Spain. In: EGU General Assembly Conference Abstracts, p. 40.

Chen, J., Cai, X., Wang, H., Kang, L., Zhang, H., Song, Y., Zhu, H., Zheng, W., Li, F., 2018. Tornado climatology of China. Int. J. Climatol. 38 (5), 2478–2489. https://doi.org/10.1002/joc.5369.

Chernokulsky, A., Shikhov, A., 2018. 1984 Ivanovo tornado outbreak: Determination of actual tornado tracks with satellite data. Atmos. Res. 207, 111–121. https://doi.org/10.1016/j.atmosres.2018.02.011.

Chernokulsky, A., Kurgansky, M., Mokhov, I., Shikhov, A., Azhigov, I., Selezneva, E., Zakharchenko, D., Antonescu, B., Kühne, T., 2020. Tornadoes in Northern Eurasia: from the Middle age to the information era. Mon. Weather Rev. 148 (8), 3081–3110. https://doi.org/10.1175/MWR-D-19-0251.1.

Cort`es, M., Turco, M., Llasat-Botija, M., Llasat, M.C., 2018. The relationship between precipitation and insurance data for floods in a Mediterranean region (Northeast Spain). Nat. Hazards Earth Syst. Sci. 18, 857–868. https://doi.org/10.5194/nhess-18-857-2018.

del Moral, A., Llasat, M.C., Rigo, T., 2017. Identification of anomalous motion of thunderstorms using daily rainfall fields. Atmos. Res. 185, 92–100. https://doi.org/10.1016/j.atmosres.2016.11.001.

del Moral, A., Weckwerth, T.M., Rigo, T., Bell, M.M., Llasat, M.C., 2020a. C-Band Dual-Doppler retrievals in complex Terrain: improving the knowledge of severe storm dynamics in Catalonia. Remote Sens. 12 (18), 2930. https://doi.org/10.3390/rs12182930.

del Moral, A., Llasat, M.C., Rigo, T., 2020b. Connecting flash flood events with radar-derived convective storm characteristics on the Northwestern Mediterranean coast: knowing the present for better future scenarios adaptation. Atmos. Res. 238, 104863. https://doi.org/10.1016/j.atmosres.2020.104863.

Donner, W.R., 2007. The political ecology of disaster: An analysis of factors influencing U.S. tornado fatalities and injuries, 1998–2000. Demography 44 (3), 669–685. https://doi.org/10.1353/dem.2007.0024.

Doswell III, C.A., Brooks, H.E., Dotzek, N., 2009. On the implementation of the enhanced Fujita scale in the USA. Atmos. Res. 93, 554–563. https://doi.org/10.1016/j.atmosres.2008.11.003.

Dotzek, N., Groenemeijer, P., Feuerstein, B., Holzer, A.M., 2009. Overview of ESSL's severe convective storms research using the European Severe Weather Database ESWD. Atmos. Res. 93, 575–586. https://doi.org/10.1016/j.atmosres.2008.10.020.

Edwards, R., LaDue, J.G., Ferree, J.T., Scharfenberg, K., Maier, C., Coulbourne, W.L., 2013. Tornado intensity estimation: past, present, and future. Bull. Am. Meteorol. Soc. 94 (5), 641–653. https://doi.org/10.1175/BAMS-D-11-00006.1.

Eidson, M., Lybarger, J.A., Parsons, J.E., Maccormack, J.N., Freeman, J.I., 1990. Risk factors for Tornado injuries. Int. J. Epidemiol. 19 (4), 1051–1056. https://doi.org/10.1093/ije/19.4.1051.

Farnell, C., Busto, M., Aran, M., Andr´es, A., Pineda, N., Tora`, M., 2009. Study of the hailstorm of 17 September 2007 at the Pla d'Urgell. Part one: fieldwork and analysis of hailpads. Tethys 6, 67–79. https://doi.org/10.3369/tethys.2009.6.05.

Farnell, C., Rigo, T., Pineda, N., 2017. Lightning jump as a nowcast predictor: Application to severe weather events in Catalonia. Atmos. Res. 183, 130–141. https://doi.org/10.1016/j.atmosres.2016.08.021.

Fujita, T.T., 1981. Tornadoes and downbursts in the context of generalized planetary scales. J. Atmos. Sci. 38 (8), 1511–1534. https://doi.org/10.1175/1520-0469(1981)038<1511:TADITC>2.0.CO;2.

Galway, J.G., 1975. Relationship of Tornado deaths to severe weather watch areas. Mon. Weather Rev. 103, 737–741. https://doi.org/10.1175/1520-0493(1975)103<0737:ROTDTS>2.0.CO;2.

Galway, J.G., 1977. Some climatological aspects of tornado outbreaks. Mon. Weather Rev. 105, 477–484. https://doi.org/10.1175/1520-0493(1977)105<0477:SCAOTO>2.0.CO;2.

Gaya`, M., 2007. The 1886 tornado of Madrid. Atmos. Res. 83 (2–4), 201–210. https://doi.org/10.1016/j.atmosres.2005.10.017.

Gaya`, M., 2018. Els Fiblons a Espanya: Climatologia i cata`leg de Tornados i Trombes (Whirlwinds in Spain: Climatology and Catalogue of Tornadoes and Waterspouts), Second edition. Universitat de les Illes Balears. (619 pp. in Catalan).

Gaya`, M., Llasat, M.C., Arús, J., 2011. Tornadoes and waterspouts in Catalonia (1950–2009). Nat. Hazards Earth Syst. Sci. 11, 1875–1883. https://doi.org/10.5194/nhess-11-1875-2011.

Goliger, A.M., Milford, R.V., 1998. A review of worldwide occurrence of tornadoes. J. Wind Eng. Ind. Aerodyn. 74–76, 111–121. https://doi.org/10.1016/S0167-6105(98)00009-9.

Gonzalez, S., Callado, A., Werner, E., Escriba`, P., Bech, J., 2018. Coastally trapped disturbances caused by the tramontane wind on the northwestern Mediterranean: numerical study and sensitivity to short-wave radiation. Q. J. R. Meteorol. Soc. 144 (714), 1321–1336. https://doi.org/10.1002/qj.3320.

Grasso, V., Zaza, I., Zabini, F., Pantaleo, G., Nesi, P., Crisci, A., 2017. Weather events identification in social media streams: tools to detect their evidence in Twitter. Peer J. Preprints 5. https://doi.org/10.7287/peerj.preprints.2241v2 e2241v2.

Grieser, J., Haines, P., 2020. Tornado risk climatology in Europe. Atmosphere 11 (7), 768. https://doi.org/10.3390/atmos11070768.

Groenemeijer, P., Kühne, T., 2014. A climatology of Tornadoes in Europe: results from the European severe weather database. Mon. Weather Rev. 142, 4775–4790. https://doi.org/10.1175/MWR-D-14-00107.1.

Guti´errez, D., Riesco, J., Ponce, S., 2015. SINOBAS, a tool for collaborative mapping applied to observation of "singular" weather phenomena. In: 15th EMS Annual Meeting & 12th European Conference on Applications of Meteorology: EMS2015-413.

Hagemeyer, B.C., 1997. Peninsular florida Tornado outbreaks. Weather Forecast. 12, 399–427. https://doi.org/10.1175/1520-0434(1997)012<0399:PFTO>2.0.CO;2.

Holzer, A.M., Schreiner, T.M.E., Pú˘cik, T., 2018. Forensic re-analysis of one of the deadliest European tornadoes. Nat. Hazards Earth Syst. Sci. 18, 1555–1565. https://doi.org/10.5194/nhess-18-1555-2018.

Homar, V., Romero, R., Ramis, C., Alonso, S., 2002. Numerical study of the October 2000 torrential precipitation event over eastern Spain: analysis of the synoptic-scale stationarity. Ann. Geophys. 20, 2047–2066.

Homar, V., Gay`a, M., Romero, R., Ramis, S., Alonso, S., 2003. Tornadoes over complex terrain: an analysis of the 28th August 1999 tornadic event in eastern Spain. Atmos. Res. 67–68, 301–317. https://doi.org/10.1016/S0169-8095(03)00064-4.

Hyv¨arinen, O., Saltikoff, E., 2010. Social media as a source of meteorological observations. Mon. Weather Rev. 138, 3175–3184. https://doi.org/10.1175/2010MWR3270.1.

IDESCAT, 2020. Official Statistics of Catalonia. https://www.idescat.cat/?lang=en (last access 21 August 2020).

Kahraman, A., Markowski, P.M., 2014. Tornado climatology of Turkey. Mon. Weather Rev. 142, 2345–2352. https://doi.org/10.1175/MWR-D-13-00364.1.

Karstens, C.D., Samaras, T.M., Gallus, W.A., Finley, C.A., Lee, B.D., 2010. Analysis of near-surface wind flow in close proximity to tornadoes. In: 25th Conference on Severe Local Storms. P10.12. Available online at. http://ams.confex.com/ams/pdfpapers/176188.pdf.

Kirk, P.J., 2014. An updated tornado climatology for the UK: 1981–2010. Weather 69 (7), 171–175.

Koch, P., Wernli, H., Davies, H.C., 2006. An event-based jet-stream climatology and typology. Int. J. Climatol. 26 (3), 283–301. https://doi.org/10.1002/joc.1255.

Kühne, T., Kollmohr, A., Hubrig, M., S¨avert, T., Schlenczek, O., Simon, W., Wichmann, H., 2017. Statistical analysis of the spatial and temporal distribution of tornadoes in Germany. In: 9th European Conference on Severe Storms: ECSS2017-132.

Leita˜o, P., Pinto, P., 2020. Tornadoes in Portugal: an overview. Atmosphere 11, 679. https://doi.org/10.3390/atmos11070679.

Lo´pez, J.M., 2007. A Mediterranean derecho: Catalonia (Spain), 17th August 2003. Atmos. Res. 83 (2–4), 272–283. https://doi.org/10.1016/j.atmosres.2005.08.008.

Mahieu, P., Wesolek, E., 2016. Tornado Rating in Europe with the EF-scale, KERAUNOS, 65 pp., available at. http://www.keraunos.org/tornado-rating-in-europe-with-the-enhanced-fujita-scale.pdf (last access: 20 August 2020).

Markowski, P.M., Richardson, Y.P., 2009. Tornadogenesis: our current understanding, forecasting considerations, and questions to guide future research. Atmos. Res. 93 (1–3), 3–10. https://doi.org/10.1016/j.atmosres.2008.09.015.

Martín, Y., Cívica, M., Pham, E., 2020. Constructing a supercell database in Spain using publicly available two-dimensional radar images and citizen science. Ann. Am. Assoc. Geogr. 1–21 https://doi.org/10.1080/24694452.2020.1812371 (In press).
Martínez-Gomariz, E., Guerrero-Hidalga, M., Russo, B., Yubero, D., Go´mez, M., Casta´n, S., 2019. Development and application of depth damage and sealing coefficient curves to estimate urban flooding economic impact on Spanish urban areas. Ingeniería del Agua 23 (4), 229–245. https://doi.org/10.4995/ia.2019.12137.
Martínez-Gomariz, E., Forero-Ortiz, E., Guerrero-Hidalga, M., Casta´n, S., Go´mez, M., 2020. Flood depth-damage curves for Spanish Urban areas. Sustainability 12 (7), 2666. https://doi.org/10.3390/su12072666.
Mateo, J., Ballart, D., Brucet, C., Aran, M., Bech, J., 2009. A study of a heavy rainfall event and a tornado outbreak during the passage of a squall line over Catalonia. Atmos. Res. 93 (1–3), 131–146. https://doi.org/10.1016/j.atmosres.2008.09.030.
Matsangouras, I.T., Pytharoulis, I., Nastos, P.T., 2014a. Numerical modeling and analysis of the effect of complex Greek topography on tornadogenesis. Nat. Hazards Earth Syst. Sci. 14 (7), 1905–1919. https://doi.org/10.5194/nhess-14-1905-2014.
Matsangouras, I.T., Nastos, P.T., Bluestein, H.B., Sioutas, M.V., 2014b. A climatology of tornadic activity over Greece based on historical records. Int. J. Climatol. 34 (8), 2538–2555. https://doi.org/10.1002/joc.3857.
Matsangouras, I.T., Nastos, P.T., Pytharoulis, I., 2016. Study of the tornado event in Greece on March 25, 2009: Synoptic analysis and numerical modeling using modified topography. Atmos. Res. 169 (B), 566–583. https://doi.org/10.1016/j.atmosres.2015.08.010.
Matsangouras, I.T., Nastos, P.T., Bluestein, H.B., Pytharoulis, I., Papachristopoulou, K., Miglietta, M.M., 2017. Analysis of waterspout environmental conditions and of parent-storm behaviour based on satellite data over the southern Aegean Sea of Greece. Int. J. Climatol. 37 (2), 1022–1039. https://doi.org/10.1002/joc.4757.
Miglietta, M.M., 2019. Waterspouts: a Review. Reference Module in Earth Systems and Environmental Sciences. https://doi.org/10.1016/B978-0-12-409548-9.12414-5.
Miglietta, M.M., Matsangouras, I.T., 2018. An updated "climatology" of tornadoes and waterspouts in Italy. Int. J. Climatol. 38, 3667–3683. https://doi.org/10.1002/joc.5526.
Miglietta, M.M., Rotunno, R., 2016. An EF3 multivortex tornado over the ionian region: is it time for a dedicated warning system over italy? Bull. Am. Meteorol. Soc. 97, 337–344. https://doi.org/10.1175/BAMS-D-14-00227.1.
Miglietta, M.M., Arai, K., Kusunoki, K., Inoue, H., Adachi, T., Niino, H., 2020. Observational analysis of two waterspouts in northwestern Italy using an OPERA Doppler radar. Atmos. Res. 234, 104692. https://doi.org/10.1016/j.atmosres.2019.104692.
Molthan, A.L., Bell, J.R., Cole, T.A., Burks, J.E., 2014. Satellite-based identification of tornado damage tracks from the 27 April 2011 severe weather outbreak. J. Oper. Meteor. 2 (16), 191–208. https://doi.org/10.15191/nwajom.2014.0216.
Molthan, A.L., Schultz, L.A., McGrath, K.M., Burks, J.E., Camp, J.P., Angle, K., Bell, J.R., Jedlovec, G.J., 2020. Incorporation and use of earth remote sensing imagery within the NOAA/NWS damage assessment toolkit. Bull. Am. Meteorol. Soc. 101, E323–E340 (doi.10.1175).
NOAA/SPC, 2019. U.S. Tornadoes (1950–2018). https://www.spc.noaa.gov/wcm/ (last access 17 February 2020).
Pastor, F., Valiente, J.A., Palau, J.L., 2018. Sea surface temperature in the mediterranean: trends and spatial patterns (1982–2016). Pure Appl. Geophys. 175 (11), 4017–4029. https://doi.org/10.1007/978-3-030-11958-4_18.
Pautz, M.E., 1969. Severe Local Storms Occurrences, 1955–1967. ESSA Tech. Memo. WBTM FCST12, Washington, DC (77 pp).
Pen˜a, J.C., Aran, M., Cunillera, J., Amaro, J., 2011. Atmospheric circulation patterns associated with strong wind events in Catalonia. Nat. Hazards Earth Syst. Sci. 11, 145–155. https://doi.org/10.5194/nhess-11-145-2011.
Pineda, N., Montany`a, J., 2009. Lightning detection in Spain: The particular case of Catalonia. In: Betz, H.-D., Schumann, U., Laroche, P. (Eds.), Lightning: Principles, Instruments and Applications. Springer, pp. 161–185.
Pineda, N., Soler, X., 2015. The influence of the Mediterranean Sea on the annual lightning distribution in Catalonia. In: 5th International Conference on Meteorology and Climatology of the Mediterranean, pp. 36–37.
Pineda, N., Bech, J., Rigo, T., Montany`a, J., 2011. A Mediterranean nocturnal heavy rainfall and tornadic event. Part II: Total lightning analysis. Atmos. Res. 100 (4), 638–648. https://doi.org/10.1016/j.atmosres.2010.10.027.
Potvin, C.K., Broyles, C., Skinner, P.S., Brooks, H.E., Rasmussen, E., 2019. A Bayesian hierarchical modeling framework for correcting reporting bias in the U.S. Tornado database. Weather Forecast. 34, 15–30. https://doi.org/10.1175/WAF-D-18-0137.1.
Ramis, C., Lo´pez, J., Arús, J., 1999. Two cases of severe weather in Catalonia (Spain). A diagnostic study. Meteorol. Appl. 6 (1), 11–27. https://doi.org/10.1017/S1350482799000869.
Rauhala, J., Brooks, H.E., Schultz, D.M., 2012. Tornado climatology of Finland. Mon. Weather Rev. 140, 1446–1456. https://doi.org/10.1175/MWR-D-11-00196.1.
Renko, T., Kuzmi´c, J., S˘oljan, V., Mahovi´c, N.S., 2016. Waterspouts in the Eastern Adriatic from 2001 to 2013. Nat. Hazards 82, 441–470. https://doi.org/10.1007/s11069-016-2192-5.
Rhee, D.M., Lombardo, F.T., 2018. Improved near-surface wind speed characterization using damage patterns. J. Wind Eng. Ind. Aerodyn. 180, 288–297. https://doi.org/10.1016/j.jweia.2018.07.017.
Rigo, T., Farnell, C., 2019. Using maximum Vertical Integrated Liquid (VIL) maps for identifying hail-affected areas: an operative application for agricultural purposes. Tethys 16, 15–24. https://doi.org/10.3369/tethys.2019.16.02.
Ripoll, R., del Amo, X., Vendrell, R., 2016. The weather observers network of the Meteorological Service of Catalonia. In: WMO Technical Conference on Meteorological and Environmental Instruments and Methods of Observation (CIMO TECO 2016). P2(57).
Rodríguez, O., Bech, J., 2018. Sounding-derived parameters associated with tornadic storms in Catalonia. Int. J. Climatol. 38, 2400–2414 (doi.1002/joc.5343).
Rodríguez, O., Bech, J., 2020a. Tornadic environments in the Iberian Peninsula and the Balearic Islands based on ERA5 reanalysis. Int. J. Climatol. 1–21 https://doi.org/10.1002/joc.6825 (In press).
Rodríguez, O., Bech, J., 2020b. Reanalysing strong-convective wind damage paths using high-resolution aerial images. Nat. Hazards 104, 1021–1038. https://doi.org/10.1007/s11069-020-04202-6.
Rodríguez, O., Bech, J., Casta´n, S., Arús, J., 2018. El Tornado del 7 de Gener de 2018: de l'Alt Empord`a al Rossello´. Treball de Camp i an`alisi de les Destrosses (the 7 January 2018 Tornado: From Alt Emporda` to Rossello´. Fieldwork and Damage Analysis). XXIV Jornades de Meteorologia Eduard Fontser`e, p. 140 (in Catalan).
Rodríguez, O., Bech, J., Soriano, J.D., Guti´errez, D., Casta´n, S., 2020. A methodology to conduct wind damage field surveys for high-impact weather events of convective origin. Nat. Hazards Earth Syst. Sci. 20 (5), 1513–1531. https://doi.org/10.5194/nhess-20-1513-2020.
Romanic, D., Refan, M., Wu, C.H., Michel, G., 2016. Oklahoma tornado risk and variability: a statistical model. Int. J. Disast. Risk Re. 16, 19–32. https://doi.org/10.1016/j.ijdrr.2016.01.011.
Romero, R., Doswell, C.A., Ramis, C., 2000. Mesoscale numerical study of two cases of long-lived quasi-stationary convective systems over Eastern Spain. Mon. Weather Rev. 128, 3731–3751. https://doi.org/10.1175/1520-0493(2001)129<3731:MNSOTC>2.0.CO;2.
Saltikoff, E., Tuovinen, J.P., Kotro, J., Kuitunen, T., Hohti, H., 2010. A climatological comparison of radar and ground observations of hail in Finland. J. Appl. Meteorol. Climatol. 49 (1), 101–114. https://doi.org/10.1175/2009JAMC2116.1.
Schuster, S.S., Blong, R.J., Speer, M.S., 2005. A hail climatology of the greater Sydney area and New South Wales, Australia. Int. J. Climatol. 25 (12), 1633–1650. https://doi.org/10.1002/joc.1199.
Shikhov, A., Chernokulsky, A., 2018. A satellite-derived climatology of unreported tornadoes in forested regions of Northeast Europe. Remote Sens. Environ. 204, 553–567. https://doi.org/10.1016/j.rse.2017.10.002.
Sioutas, M.V., 2011. A tornado and waterspout climatology for Greece. Atmos. Res. 100 (4), 344–356. https://doi.org/10.1016/j.atmosres.2010.08.011.
Sioutas, M., Doe, R.K., 2019. Significant tornado and strong waterspout climatology of Greece. In: 10th European Conference on Severe Storms: ECSS2019-214.
Sioutas, M., Szilagyi, W., Keul, A., 2013. Waterspout outbreaks over areas of Europe and North America: Environment and predictability. Atmos. Res. 123, 167–179. https://doi.org/10.1016/j.atmosres.2012.09.013.
Taszarek, M., Brooks, H.E., Czernecki, B., 2017. Sounding-derived parameters associated with convective hazards in Europe. Mon. Weather Rev. 145, 1511–1528. https://doi.org/10.1175/MWR-D-16-0384.1.
Taszarek, M., Allen, J.T., Pú˘cik, T., Hoogewind, K.A., Brooks, H.E., 2020. Severe convective storms across Europe and the United States. Part II: ERA5 environments associated with Lightning, large hail, severe wind, and tornadoes. J. Clim. 33, 10263–10286. https://doi.org/10.1175/JCLI-D-20-0346.1.
Verbout, S.M., Brooks, H.E., Leslie, L.M., Schultz, D.M., 2006. Evolution of the U.S. Tornado Database: 1954–2003. Weather Forecast. 21, 86–93. https://doi.org/10.1175/WAF910.1.
Wakimoto, R.M., Wilson, J.W., 1989. Non-supercell tornadoes. Mon. Weather Rev. 117 (6), 1113–1140. https://doi.org/10.1175/1520-0493(1989)117<1113:NST>2.0.CO;2.
Wegener, A., 1917. Wind- Und Wasserhosen in Europa (Tornadoes and Waterspouts in Europe). Vieweg (301 pp).
Wilson, J., Carbone, R., Baynton, H., Serafin, R., 1980. Operational application of meteorological doppler radar. Bull. Am. Meteorol. Soc. 61, 1154–1168. https://doi.org/10.1175/1520-0477(1980)061<1154:OAOMDR>2.0.CO;2.
WSEC, 2006. A Recommendation for an Enhanced Fujita Scale (EF-scale). http://www.spc.noaa.gov/faq/tornado/EFScale.pdf (last access 21 August 2020).
Wurman, J., Kosiba, K., Robinson, P., Marshall, T., 2014. The role of multiple-vortex tornado structure in causing storm researcher fatalities. Bull. Am. Meteorol. Soc. 95 (1), 31–45. https://doi.org/10.1175/BAMS-D-13-00221.1.
Zrni´c, D.S., Burgess, D.W., Hennington, L.D., 1985. Automatic detection of mesocyclonic shear with doppler radar. J. Atmos. Ocean. Technol. 2, 425–438. https://doi.org/10.1175/1520-0426(1985)002<0425:ADOMSW>2.0.CO;2.